4/78 | CMCRCZ 7 (4), 169-236 (1978)

ΧΗΜΙΚΑ ΧΡΟΝΙΚΑ

ΝΕΑ ΣΕΙΡΑ

CHIMIKA CHRONIKA

NEW SERIES

AN INTERNATIONAL EDITION
OF THE GREEK CHEMISTS ASSOCIATION

CHIMIKA CHRONIKA, NEW SERIES Volume 7, No 4, pp. 169-236, December 1978

ΧΗΜΙΚΑ ΧΡΟΝΙΚΑ

ΝΕΑ ΣΕΙΡΑ

CHIMIKA CHRONIKA

NEW SERIES

1978

VOLUME 7

VOLUME'S CONTENTS

Issue No 1,

Issue No 2,

Issue No 3,

Issue No 4

CHIMIKA CHRONIKA / NEW SERIES
Published by the Greek Chemists' Association
27, Kaningos Street, Athens (147), Greece

Correspondence, submission of papers, subscriptions, renewals and changes of address should be sent to Chimika Chronica, New Series, 27 Kaningos street, Athens 147, Greece. Subscriptions are taken by volume at 300 drachmas for members and 500 drachmas for Corporations in Greece and 15 U.S. dollars to all other countries except Cyprus, where subscriptions are made on request.
Printed in Greece by Boukouris' Grafics.
Ὑπεύθυνος συμφώνως τῷ νόμῳ: Βασιλ. Καπούλας, Παπαδιαμάντη 25, Παλ. Ψυχικό, Ἀθῆναι. *Ὑπεύθυνος Τυπογραφείου:* Α. Μπούκουρης, Ποταμοῦ καί Αὐγῆς (17° χλμ. Ἐθν. Ὁδοῦ Ἀθηνῶν - Λαμίας), Νέα Κηφισιά.

CHIMIKA CHRONIKA, *NEW SERIES*

CONTENTS

Chimika Chronika, New Series. 7, 171-178 (1978)

ÉTUDE CHIMIQUE DE QUELQUES DÉRIVÉS DE L'IMIDAZO [2,1-b] THIAZOLE ET IMIDAZO [2,1-b] BENZOTHIAZOLE, D'UN INTÉRÊT PHARMACOLOGIQUE. (*)

E. COSTAKIS, M. HAMOGEORGAKIS et G. TSATSAS
Laboratoire de Chimie Pharmaceutique, Université d'Athènes, Athènes, Grèce.
(Reçu le 20 Septembre 1977)

Résumé

Le présent travail comprend la synthèse et l'étude spectroscopique (U.V., I.R. et R.M.N.) de quelques dérivés contenant les systèmes rigides suivants: le bicyclique imidazo [2,1-b] thiazole et le systéme tricyclique imidazo [2,1-b] benzothiazole.

La même étude comprend aussi la synthèse d'un nouveau noyau hétérocyclique, la dihydro- 2,3 imidazo [2,1-b] benzothiazolone-2

Les produits synthétisés sont d'un intérêt pharmacologique qui semble s'attacher à la présence du système S-C(=N)-N du type amidine dans leurs molécules.

Introduction

Ce travail fait partie d'une plus large recherche des structures caractérisées par la présence du squelette de l'amino-2thiazole dans le but d'obtenir des substances d'un intérêt pharmacologique. Récemment, nous avons découvert que les dérivés alcoylaminoacylamino- et alcoylaminoacylimino- de l'amino-2 benzothiazole et imino-2 méthyl-3 benzothiazoline respectivement, présentent des activités biologiques intéressantes.[1] Il faut y ajouter que certains composés contenant le système bicyclique rigide sous question se sont révélés d'un intérêt pharmacologique remarquable (Tetramisole)[2] et qu'un nombre des composés relatifs qui contiennent comme partie caractéristique fondamentale le système S-C(=N)-N qui rappèlle celui des amidines,[4,5] présentent une action différente utile au point de vue biologique.[3]

La présence et probablement la relation de cette partie de la molécule avec l'action biologique de ces substances nous a poussé à la synthèse des dits dérivés dont la structure est représentée par les formules 1, 2, 3 et 4.

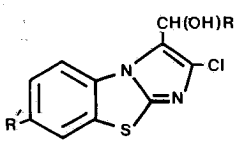

1

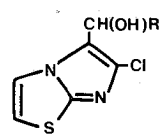

2

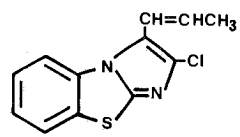

3

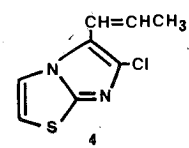

4

Dans une précédente publication que nous avons réalisée[1,6] nous exposons

(*) Les résultats concernant l'étude pharmacologique seront publiés quand cette étude sera complétée.

la synthèse des composés hétérocycliques du type 5(n=2 ou 3) qui sont obtenus en traitant respectivement en milieu alcalin le β- chloropropionylamino- et le γ-chlorobutyrylamino-2 benzothiazole. Malheureusement un traitement semblable du chloracétylamino-2 benzothiazole fournit des polymères.

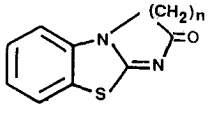

5 (n=2 ou 3)

La dihydro-2,3 imidazo [2,1-b] benzothiazolone-2(7) a été préparée à partir de l'imino-2 carbéthoxyméthyl-3 benzothiazoline (6)[7,8] par action de l'éthylate de sodium.

En faisant agir le $POCl_3$ sur le 7 nous avons obtenu le chloro-2-imidazo [2,1-b] benzothiazole (9a). Ce produit a été aussi synthétisé par Parrick et Pearson,[9] par hydrolyse acide de l'ester 6, transformation de l'acide formé en son sel de sodium et action du $POCl_3$ sur ce dernier. Afin de synthétiser le 9a nous avons finalement utilisé une voie plus rapide: En faisant réagir le chloracétate de sodium avec l'amino-2-benzothiazole[8,9] nous obtenons l'imino-2-carboxyméthyl-3-benzothiazoline (8a) qui sous l'influence de $POCl_3$ donne le chloro-2-imidazo [2,1-b] benzothiazole (9a)

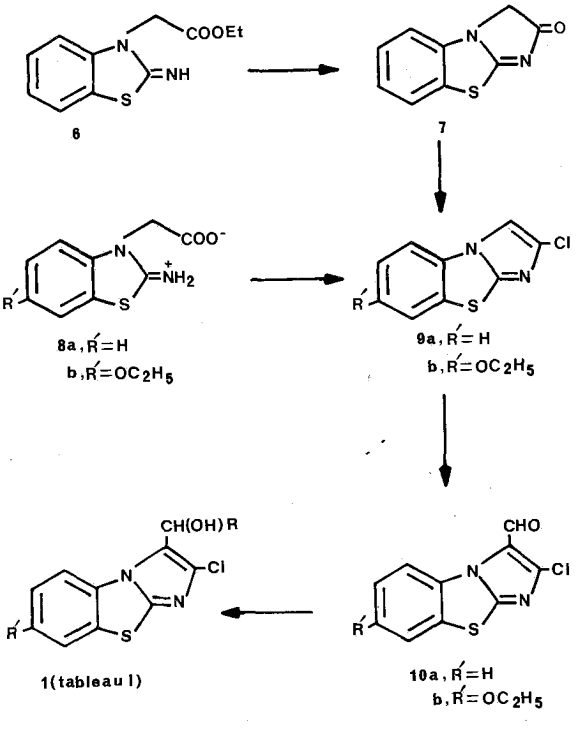

La sensibilité de la position -3 du composé 9a vis à vis d'une attaque électrophile[10] nous a permis de synthétiser facilement l'aldéhyde 10 a en utilisant

la réaction de Vilsmeier-Haack. Enfin en faisant réagir les réactifs de Grignard appropriés sur l'aldéhyde 10a nous avons préparé les dérivés du type 1 (R' H) substitués en position -3. Les conditions réactionnelles sont données dans la partie expérimentale et le tableau I, les rendements et les constantes physiques dans le tableau I (No 1-8).

À partir de l'amino-2-carboxyméthyl-3-éthoxy-6-benzothiazoline (8b) nous préparons d'une manière analogue (8b → 9b → 10b) les dérivés du type 1, R' = OC_2H_5. Les rendements et les constantes physiques sont mentionnés dans le tableau I (no 9-16).

Le chloro-6-carboxaldéhyde-5-imidazo [2,1-b] thiazole qui a été utilisé pour la préparation des dérivés du type 2 substitués en position -5 a été obtenu à partir de l'imino-2-carboxyméthyl-3-thiazoline, selon Paolini et Lendvay.[10] Les produits de la réaction du chloro-6-carboxaldéhyde-5-imidazo [2,1-b] thiazole avec les différents réactifs de Grignard sont indiqués dans le tableau II ainsi que leurs rendements et leurs constantes physiques.

Les dérivés styréniques 3 et 4 ont été préparés en chauffant à l'ébullition dans l'acétone, en présence d'iode comme catalyseur, les chloro-2(hydroxy-1propyl)-3-imidazo [2,1-b] benzothiazole et chloro-6 (hydroxy-1propyl)-5-imidazo [2,1-b] thiazole respectivement. Les rendements respectifs que nous avons atteint pour les composés 3 et 4 en utilisant cette déshydratation où le rôle de l'iode n'a pas encore été éclairci, [11,12,13]sont de l'ordre de 94%et 72%.

Les analyses élèmentaires mises à part, les spectres U.V., I.R. et R.M.N., sont également en accord avec des structures des substances préparées. Dans la partie expérimentale nous en exposons des exemples représentatifs.

Ce qui caractérise presque tous les spectres R.M.N. des composés du type 1 et 2 est un lent transfert du proton de l'hydroxyle; le signal de ce proton se présente comme un doublet, tandis que le signal du groupement methine se présente (suivant le derivé) comme un doublet et d'habitude comme un multiplet. Tous les spectres ont été obtenus dans la DMSO deuterée ou le $CDCI_3$ à la température ambiante.

Partie Expérimentale

Les températures de fusion ont été obtenues en utilisant l'appareil de Büchi et ne sont pas corrigées.

Les spectres I.R. ont été enregistrés à l'aide d'un spectrophotomètre Perkin-Elmer modèle 177, en pastille de KBr, et les spectres U.V. à l'aide d'un appareil Perkin-Elmer 137 UV dans l'éthanol.

Les spectres R.M.N. ont été enregistrés sur un appareil Varian A60; les déplacements chimiques sont donnés en δ(p.p.m.) par rapport au TMS comme référence interne. Dans le texte: s: singulet, d: doublet, t:triplet, q: quadruplet, m: multiplet.

Les microanalyses ont été effectuées par le Service Central de Microanalyse de C.N.R.S., que nous remercions vivement.

Dihydro-2,3 imidazo [2,1-b] benzothiazolone-2 (7).

Dans une solution de 11,8g (0,05 mole) d'imino-2-carbéthoxyméthyl-3-benzothiazoline (6) dans 200 ml de EtOH on ajoute sous agitation 3,4g (0,05 mole) de EtONa en solution dans 200 ml de EtOH et le mélange est laissé pendant 30 min à la température ambiante. Après avoir éliminé l'éthanol sous pression réduite, on traite le résidu par un petit volume d'eau froide, on ajoute 1 ml d'acide acétique et on filtre. On traite le précipité obtenu trois fois avec de

TABLEAU I

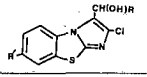

N°	R'	R	HALOGENE D'ALKYLE ou D'ARYLE (MOLES)**	F°C	Rdt%	Analyses Calc.% C	H	N	S	Tr. % C	H	N	S
1	H	CH_3	CH_3J(0,04)	149-150	59	52,27	3,59	11,08	12,69	51,99	3,65	11,07	12,75
2	H	CH_2CH_3	C_2H_5Br (0,04)	181-182	65	54,03	4,16	10,50	12,02	54,05	4,17	10,58	12,24
3	H	$CH(CH_3)_2$	i-C_3H_7Br(0,06)	218-220	23	55,60	4,66	9,98	11,42	55,86	4,77	9,95	11,33
4	H	$C(CH_3)_3$	t-C_4H_9Cl(0,1)	220-221	39	57,04	5,13	9,50	10,88	57,24	5,16	9,50	10,96
5	H	C_6H_5	C_6H_5Br(0,06)	200-201	84	61,04	3,52	8,90	10,19	61,30	5,56	8,82	10,23
6	H	0-CH_3-C_6H_4	0-CH_3-C_6H_4Br(0,06)	213-214*	67	62,09	3,98	8,52	9,76	62,10	4,13	8,31	9,63
7	H	m-CH_3-C_6H_4	m-CH_3-C_6H_4Br(0,06)	200-201	60	62,09	3,98	8,52	9,76	62,33	4,01	8,30	9,76
8	H	p-CH_3-C_6H_4	p-CH_3-C_6H_4Br(0,06)	208-210	56	62,09	3,98	8,52	9,76	61,93	3,97	8,69	9,54
9	OC_2H_5	CH_3	CH_3J(0,04)	173-174*	26	52,61	4,41	9,44	10,81	52,89	4,30	9,45	10,77
10	OC_2H_5	CH_2CH_3	C_2H_5Br(0,04)	153-154	40	54,09	4,86	8,95	10,31	54,26	4,96	9,12	10,39
11	OC_2H_5	$CH(CH_3)_2$	i-C_3H_7Br(0,08)	181-182	41	55,46	5,27	8,62	9,88	55,57	5,48	8,65	9,77
12	OC_2H_5	$C(CH_3)_3$	t-C_4H_9Cl(0,12)	200-201	39	56,70	5,65	8,27	9,56	56,78	5,83	8,33	9,58
13	OC_2H_5	C_6H_5	C_6H_5Br(0,07)	196-197*	63	60,24	4,21	7,80	8,94	60,39	4,35	7,70	8,80
14	OC_2H_5	0-CH_3-C_6H_4	0-CH_3-C_6H_4Br(0,07)	238-240*	60	61,20	4,59	7,51	8,60	61,41	4,54	7,40	8,39
15	OC_2H_5	m-CH_3-C_6H_4	m-CH_3-C_6H_4Br(0,07)	204-205*	60	61,20	4,59	7,51	8,60	61,60	4,61	7,56	8,57
16	OC_2H_5	p-CH_3-C_6H_4	p-CH_3-C_6H_4Br(0,07)	206-207*	53	61,20	4,59	7,51	8,60	61,08	4,63	7,38	8,58

* Fusion avec décomposition ** Moles du dérivé halogéné pour 0,03 mole d'aldéhyde.

TABLEAU II

N°	R	HALOGENE D'ALKYLE ou D'ARYLE (MOLES)*	F°C	Rdt%	Analyses Calc.% C	H	N	S	Tr.% C	H	N	S
1	CH_3	CH_3J(0,04)	108-109	40	41,48	3,48	13,82	15,82	41,77	3,51	13,76	15,46
2	CH_2CH_3	C_2H_5Br(0,04)	118-119	67	44,34	4,19	12,93	14,80	44,59	4,32	13,06	14,55
3	$CH(CH_3)_2$	i-C_3H_7Br(0,06)	138-139	57	46,85	4,80	12,14	13,90	46,61	4,66	12,01	13,67
4	$C(CH_3)_3$	t-C_4H_9Cl(0,1)	152-153	54	49,07	5,35	11,45	13,10	49,03	5,55	11,57	13,21
5	C_6H_5	C_6H_5Br(0,06)	147-148	80	54,45	3,42	10,58	12,11	54,53	3,43	10,38	12,10
6	o-CH_3-C_6H_4	o-CH_3-C_6H_4Br(0,06)	199-200	59	56,03	3,97	10,06	11,50	56,20	3,97	9,76	11,43
7	m-CH_3-C_6H_4	m-CH_3-C_6H_4Br(0,06)	180-181	65	56,03	3,97	10,06	11,50	56,30	4,06	9,78	11,68
8	p-CH_3-C_6H_4	p-CH_3-C_6H_4Br(0,06)	176-177	84	56,03	3,97	10,06	11,50	56,32	4,11	9,66	11,49

* Moles du dérivé halogéné pour 0,03 mole d'adléhyde.

l'eau chaude (120 ml en tout), en filtrant après chaque traitement. Après refroidissement des filtrats réunis, le composé 7 précipite. On recristallise dans un mélange éthanol-éther. F déc. = 213-214° C. Rdt = 78%.

Analyse $C_9H_7N_2OS$: Calc. % : C 56,52 H 3,69 N 14,65.
Tr. % : C 56,66 H 3,29 N 14,62

Spectre I.R. (KBr): ν (C=0) 1710 cm^{-1}

Spectre R.M.N. (DMSO-d_6): δ = 4,61 p.p.m. (s, 2H, -CH_2-); 7,10-8,20 p.p.m. (m, 4H aromatiques).

Chloro-2-imidazo [2,1-b] benzothiazole (9a)

Méthode A.

Dans 7,65g (0,04 mole) de 7 on ajoute 40 ml de $POCl_3$ et le mélange est chauffé à reflux pendant 4h. Après avoir éliminé le $POCl_3$ sous pression réduite, le résidu est versé dans l'eau froide et alcalinisé avec du NaOH à 10%. Le précipité formé est filtré et recristallisé dans l'éthanol. F=163-164°C. [Litt.[7] F=164-165°C]. Rdt=70%.

Méthode B

Dans une solution de 15g (0,1 mole) d'amino-2-benzothiazole dans 50ml d'éthanol on ajoute 11,6 g (0,1 mole) de chloracétate de sodium et le mélange est chauffé à reflux pendant 24h. Après refroidissement, on filtre et sèche le précipité formé. Dans 15g d'imino-2-carboxyméthyl-3 benzothiazoline (8a) ainsi obtenue, on ajoute 50ml de $POCl_3$ et le mélange est chauffé à reflux pendant 2h. Après élimination de l'excès de $POCl_3$ on continue comme dans la méthode A. F=163-165°C (EtOH). Rdt=38% par rapport à l'amino-2-benzothiazole.

Chloro-2 éthoxy-7imidazo 2,1-b benzothiazole (9b)

En opérant d'une manière analogue à la méthode B on obtient 10g d'imino-2-carboxyméthyl-3-éthoxy-6-benzothiazoline (8b) à partir de 9,8g (0,05 mole) d'amino-2-éthoxy-6-benzothiazole et 5,8g (0,05 mole) de chloracétate de sodium. Le produit obtenu est traité par 45ml de $POCl_3$. Le produit brut obtenu 9b est purifié par chromatographie sur colonne (gel de silice, élution avec le mélange benzène-acétate d'éthyle 7:3). On recristallise dans l'éthanol, F=183-184°C. Rdt=42% par rapport à l'amino-2éthoxy-6benzothiazole.

Analyse $C_{11}H_9ClN_2OS$: Calc. % : C 52,27 H 3,59 N 11,08 Cl 14,03
Tr. % : C 52,29 H 3,79 N 11,07 Cl 13,74

Spectre R.M.N. ($CDCl_3$): 1,27 p.p.m. (t, 3H, -CH_3 éthoxyle);

3,78 p.p.m. (q, 2H, -OCH_2- éthoxyle); 7,36 p.p.m. [s, 1H, =CH-(H-3)]; 7,22-7,66 p.p.m. (m, 3H aromatiques).

Chloro-2-carboxaldéhyde-3-imidazo [2,1-b] benzothiazole (10a)

Dans un mélange de 4,8 ml de DMF avec 100 ml de $CHCl_3$ on ajoute goutte à goutte 6 ml de $POCl_3$ et ensuite en petites quantités 12,5g (0,06 mole) de chloro-2-imidazo [2,1-b] benzothiazole (9a). Le mélange est chauffé à reflux pendant 3h, puis on élimine le solvant sous pression réduite et le résidu est traité par de l'eau. Le précipité formé est filtré et recristallisé dans l'éthanol. F=176-177°C. Rdt=56%.

Analyse $C_{10}H_{15}ClN_2OS$: Calc. % : C 50,75 H 2,13 N 11,83 S 13,55.
Tr. % : C 50,58 H 2,05 N 11,63 S 13,40

Spectre I.R. (KBr): ν(C=0) 1663 cm^{-1}.

Spectre R.M.N. ($CDCl_3$):δ=7,19-7,74 p.p.m. (m,3H aromatiques);8,88-9,12 p.p.m. (m, 1H aromatique); 9,80 p.p.m. (s, 1H, -CHO).

Chloro-2-carboxaldéhyde-3-éthoxy-7-imidazo [2,1-b] benzothiazole (10b)

Nous l'avons préparé d'une manière analogue à celle du composé 10a à partir de 10g (0,04 mole) de chloro-2-éthoxy-7-imidazo [2,1-b] benzothiazole (9b), 3,2 ml de DMF, 4ml $POCl_3$, 60ml de $CHCl_3$ et chauffage pendant 3h. Recristallisation dans l'éthanol. F=196-197°C. Rdt=69%.

Analyse $C_{12}H_9ClN_2O_2S$: Calc. % : C 51,34 H 3,23 N 9,98 S 11,42
Tr. % : C 51,05 H 3,38 N 9,90 S 11,70

Spectre I.R. (KBr): ν(C=0) 1668 cm^{-1}

Spectre R.M.N. ($CDCl_3$):δ=1,2 p.p.m. (t, 3H, $-CH_3$ éthoxyle); 3,76 p.p.m. (q, 2H, $-OCH_2$-éthoxyle); 7,28-7,82 p.p.m. (m, 2H aromatiques); 8,82 p.p.m. (s, 1H aromatique); 9,77 p.p.m. (s, 1H, -CHO).

Chloro-2(hydroxy-1alcoyl ou aryl)-3-imidazo [2,1-b] benzothiazoles et chloro-2(hydroxy-1 alcoyl ou aryl)-3-éthoxy-7-imidazo [2,1-b] benzothiazoles (1).

Technique générale. On prépare l'organomagnésien à partir de 0,04 à 0,12 mole d'halogénure d'alcoyle ou d'aryle et de 0,04 à 0,12 atome-gramme de magnésium suivant l'aldéhyde (voir tableau I). On ajoute goutte à goutte dans cette quantité de réactif de Grignard en solution dans 100ml d'éther anhydre, une solution de 0,03 mole de 10a ou 10b dans 150 ml d'éther anhydre, sous agitation et refroidissement (NaCl+glace). Après addition complète on continue agiter pendant 4h à la température ambiante, puis décompose le mélange réactionnel avec 30-40ml d'eau. Après avoir séparé et séché sur Na_2SO_4 la couche étherée, on évapore le solvant et recristallise le résidu dans le benzène. Dans le tableau I on trouve les produits du type 1 préparés avec leurs constantes physiques et leurs analyses.

Chloro-6(hydroxy-1alcoyl ou aryl)-5 imidazo [2,1] thiazoles (2).

Nous les avons préparés comme les dérivés du type 1 par action de 0,04 à 0,1 mole d'halogénure d'alcoyl-ou d'aryl-magnésium suivant l'aldéhyde (voir tableau II) sur 0,03 mole de chloro-6 carboxaldéhyde-5 imidazo [2,1-b] thiazole.[10]

Dans le tableau II nous trouvons les produits préparés du type 2 avec leurs constantes physiques et leurs analyses.

Spectres représentatifs (U.V., I.R. et R.M.N.) des produits des type 1 et 2

A. *Chloro-2-(hydroxy-1propyl)-3-imidazo [2,1-b] benzothiazole, (1, R=CH_2CH_3, R'=H):*

Spectre U.V. (EtOH): λmax.=235 nm (ε=16000); 285nm (ε=3200)

Spectre I.R. (KBr): ν(OH) 3260 cm^{-1}

Spectre R.M.N. (DMSO-d_6):δ=0,91 p.p.m. (t,J=7Hz, 3H,-CH_3); 1,92 p.p.m. (qd, J=7Hz et J=3, 8Hz, 2H, -CH_2-); 4,96 p.p.m. (td, J=7Hz et J=3, 8Hz, 1H, méthine); 6,03 p.p.m. (d, J=3, 8Hz, 1H,-OH) et 7,04-8,55 p.p.m. (m, 4H aromatiques).

B. *Chloro-6(hydroxy-1néopentyl)-5-imidazo [2,1-b] thiazole, [2, R=-$C(CH_3)_3$]:*

Spectre U.V. (EtOH):λmax=255nm (ε=4800).

Spectre I.R. (KBr): ν(OH) 3280 cm^{-1}

Spectre R.M.N. (DMSO-d_6):δ=0,93 p.p.m. [s, 9H,-$C(CH_3)_3$]; 4,51 p.p.m. (d, J=4Hz, 1H, méthine); 5,75 p.p.m. (d, J=4Hz, 1H,-OH); 7,24 p.p.m. (d, J=5Hz, 1H,=CH-) et 7,80 p.p.m. (d, J=5Hz, 1H,=CH-)

C. *Chloro-6(hydroxy-1benzyl)-5-imidazo [2,1-b] thiazole, (2, R=-C_6H_5):*

Spectre U.V. (EtOH):λmax=256nm (ε=4800)

Spectre I.R. (KBr): ν(OH) 3180 cm^{-1}

Spectre R.M.N. (DMSO-d_6):δ=6,0 p.p.m (d, J=4Hz, 1H, méthine); 6,38 p.p.m. (d, J=4Hz, 1H, -OH); 7,22 p.p.m. (d, J=5Hz, 1H,=CH-); 7,32 p.p.m. (s, 5H aromatiques) et 7,57 p.p.m. (d, J=5Hz, 1H,=CH-).

Déshydratation du chloro-2(hydroxy-1 propyl)-3-imidazo [2,1-b] benzothiazole, (1, R=-CH_2CH_3, R'=H).

Dans une solution de 1g (0,004 mole) de chloro-2 (hydroxy-1propyl)-3 imidazo [2,1-b] benzothiazole dans 25 ml d'acétone, on ajoute 0,005-0,010g d'iode et on chauffe à reflux pendant 20h. On élimine l'acétone sous pression réduite et le résidu, le chloro-2(propényl-1)-3-imidazo [2,1-b] benzothiazole (3), est recristallisé dans l'éther.

F=173-175°C. Rdt=91%.

Analyse $C_{12}H_9ClN_2S$: Calc. % : C 48,36 H 3,55 N 14,11 S 16,14
Tr. % : C 48,65 H 3,49 N 14,11 S 16,06.

Spectre U.V. (EtOH):λmax=250mn (ε=17000); 297nm (ε=8000)

Spectre R.M.N. ($CDCl_3$):δ=1,97 p.p.m. (d, J=5Hz 3H, -CH_3); 5,74-6,70 p.p.m. (m. 2H, olef. -CH=CH-) et 7,14-7,78 p.p.m. (m, 4H aromatiques).

Déshydratation du chloro-6(hydroxy-1propyl)-5-imidazo [2,1-b] thiazole, (2, R=-CH_2CH_3).

A partir du chloro-6(hydroxy-1propyl)-5-imidazo [2,1-b] thiazole nous obtenons d'une manière semblable le chloro-6(propényl-1)-5-imidazo [2,1-b] thiazole. Recristallisation dans l'éther additionné de n-pentane.

F=98-99°C. Rdt=72%.

Analyse $C_8H_9ClN_2S$: Calc. % : C 57,97 H 3,62 N 11,26 S 12,89
Tr. % : C 57,76 H 3,64 N 11,31 S 12,62

Spectre U.V. (EtOH): λmax=280nm (ε=11000).

Spectre R.M.N. (DMSO-d_6):δ=1,87 p.p.m. (d, J=5Hz, 3H, -CH_3); 5,65-7,75 p.p.m. (m, 2H, olef.-CH=CH-); 7,38 p.p.m. (d, J=5Hz, 1H, thiaz.=CH-) et 8,14 P.P.M. (D, J=5Hz, 1H, thiaz.=CH-).

Περίληψις

Χημικὴ μελέτη ὁρισμένων παραγώγων τοῦ ἰμιδαζο[2,1-b]θειαζολίου καὶ ἰμιδαζο[2,1-b]βενζοθειαζολίου, φαρμακολογικοῦ ἐνδιαφέροντος.

Ἡ παροῦσα ἐργασία περιλαμβάνει τὴν σύνθεσιν καὶ τὴν φασματοσκοπικὴν μελέτην (U.V., I.R. καὶ R.M.N.) παραγώγων ἀκάμπτων δικυκλικῶν (ἰμιδαζο[2,1-b]θειαζόλιον) καὶ τρικυκλικῶν (ἰμιδαζο[2,1-b]βενζοθειαζόλιον) συστημάτων.

Εἰς τὴν μελέτην τῆς συνθέσεως αὐτῶν περιλαμβάνεται ἐπίσης καὶ ἡ σύνθεσις ἑνὸς νέου ἑτεροκυκλικοῦ πυρῆνος, τῆς 2,3-διυδρο-ιμιδαζο[2,1-b] βενζοθειαζολ-2-όνης.

Αἱ παρασκευασθεῖσαι ἑνώσεις εἶναι φαρμακολογικοῦ ἐνδιαφέροντος· ἐνδιαφέρον τὸ ὁποῖον συνδέεται μὲ τὴν παρουσίαν τοῦ «ἀμιδινικοῦ» συστήματος (S-C$\overset{N}{\underset{N}{<}}$) εἰς τὴν δομὴν αὐτῶν.

Abstract

Chemical study of some imidazo [2,1-b] thiazole and imidazo [2,1-b] bensothiazole derivatives, of a pharmacological interest (*).

The present paper describes the synthesis and spectral properties of some imidazo [2,1-b] thiazole and imidazo [2,1-b] benzothiazole derivatives, as well as the synthesis of new heterocycle, the 2,3-dihydro-imidazo [2,1-b] benzothiazol 2-one.

Bibliographie

1. Tsatsas G. et Costakis E., Praktika de l'Académie d'Athènes, **51**, 469 (1976).
2. Raeymaekers A.H., Allewijin F.T., Vandenberk J., Demoen P.J., Van Affenwert T.T. et Janssen P.A.: *J. Med. Chem.*, **9**, 545 (1966).
3. Tartler G. et Weuffen W.: *Pharmazie*, **21**, 425 (1966); Almirante L., Polo L., Mugnaini A., Drovinciali E., Rugarli P., Gamba A., Olivi A. et Murmann W.: *J. Med Chem.*, **9**, 29 (1966); Bel S.C. et Wei P.H.L.: *J. Med Chem.*, **19** 524 (1976).
4. Jen T., Dienel B., Bowman H., Helt A. et Loev B.: *J. Med. Chem.*, **15**, 725 (1972).
5. Ogura H., Takayanagi H., Yamazaki Y., Takagi H., Kobayashi S., Kamioka T. et Kamoshita K.: *J. Med. Chem.*, **15**, 923 (1972).
6. Tsatsas G. et Costakis E.: *Chem. Commun.*, 991 (1967).
7. Parrick J. et Pearson K.: *Chem. et Ind.*, 1261 (1970).
8. Allen C.F.H. et Vanallan J.A.: *J. Org. Chem.:* **13**, 603 (1948).
9. Paoloni J.P.: *J. Org. Chem.*, **33**, 888 (1968).
10. Paolini J.P. et Lendvay L.J.: *J. Med. Chem.*, **12**, 1031 (1969).
11. Fieser L.F. et Fieser M., *"Reagents for organic synthesis"*, Vol. I, p. 498, Wiley and Co, Ed., 1967.
12. Beale C.H. et Hatt H.H.: *J. Am. Chem. Soc.*, **54**, 2405 (1932).
13. Hatt H.H., Pilgrim A. et Stephenson E.F.M., *J. Chem. Soc.*, 478 (1941).

Chimika Chronika, New Series 7, 179-188 (1978)

THE INFLUENCE OF SUBSTITUENTS ON THE MECHANISM AND RATE OF THE ANODIC OXIDATION OF HYDRAZINE IN ACID SOLUTION.

PANTELIS KARABINAS and JOACHIM HEITBAUM
Laboratory of Physical Chemistry, the University of Thessaloniki, Greece.
Institute of Physical Chemistry, the University of Bonn, W. Germany
(Received October 31, 1977)

Summary

The influence of substituents (methyl-or phenyl-groups) on the mechanism and the rate of the anodic oxidation of hydrazine on Pt-electrodes in sulfuric acid is discussed by means of inductive and resonance effects. It is shown that the peak potentials E_p and the rates of the anodic processes for the different derivates vary linearly with the change of the enthalpy $\delta\Delta H_o^{\neq}$

Key words: Substituent effect, Oxidation mechanism, Hydrazine and derivatives, Apparent activation energies.

Introduction

The mechanism of the anodic oxidation of hydrazine on platinum in acid solutions in principle is a successive dehydrogenation of the molecule. This was shown to be true for hydrazine itself by Harrison and Khan[1] and for the derivates phenylhydrazine (PH),[2] methylhydrazine (MH)[3] and 1,1-dimethylhydrazine (DMH)[4] by the authors. In all cases an interference with adsorption-desorption steps occurs.

The similarity of the formation mechanism of an intermediate during the oxidation suggests a determination of the influence of the different substituents on the rate of the anodic process. This is the aim of the present work.

Experimental

The experimental methods of taking cyclic current-potential diagrams and of measuring quasistationary current-potential curves are given in a previous paper.[2] The preparation of the solutions and the activation processes of the electrodes may also be found in the literature cited.[2,3,4]

In order to obtain current-potential curves at different temperatures the H typ glass cell[2] used was carefully thermostated within ± 0.1°C. The SCE-reference electrode was held at the same temperature and the temperature dependence of its potential was taken into account.[5]

Results

Fig. 1 shows, for a comparison, the current-potential scan diagrams of hydrazine and its derivates mentioned. Always the first sweep on a freshly activated electrode is given.

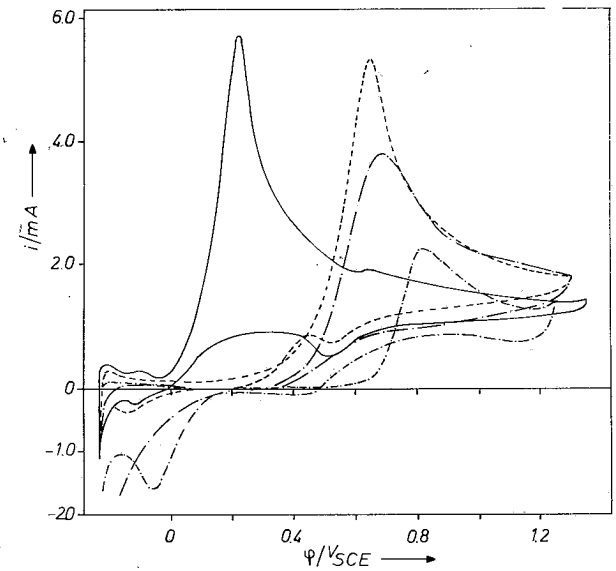

FIG. 1: *Current potential diagrams of different hydrazine derivates (5.10^{-3} M) in 1 M H_2SO_4 on Pt.v=100 mV s^{-1}, T = 25°C, deaerated solution.*
——H_2NNH_2,----CH_3NHNH_2,—·—·—·—$C_6H_5NHNH_2$,-·-·-·-·-·-$(CH_3)_2NNH_2$

In the cases of PH and DMH reducible intermediates are formed as can be seen from Figs. 2 and 3, respectively. In fig. 3, the DMH was oxidized on a Pt-disc electrode by taking cyclic potential diagrams with different anodic reverse potentials and the intermediate was reduced on the Pt-ring at a constant potential of φ_R = -75 mV_{SCE}. The current ratio $|i_R| / i_D$ in Fig. 3 corresponds to the collection efficiency N=0.32, calculated from the electrode geometry.

In the case of MH the reduction peak was found to be too small to be investigated. Hydrazine itself shows no reduction peak at all under the experimental conditions applied.

For all compounds under investigation Tafel lines were obtained at different temperatures. Respective examples are given in Fig. 4. In all cases the Tafel slopes were independent of temperature within the limits of error. This is consistent with theoretical considerations[22] which predict a temperature dependence of the transfer coefficient but only in a measurable quantity for large temperature intervals.

Plots of log i at any constant potential against 1/T proved to be straight lines as shown in Fig. 5 and from the different slopes the apparent energies of activation for the respective oxidation reactions were calculated.

In order to demonstrate the method, the equation for the calculation of $\Delta H_o^{\neq}$ shall be given for the case of PH. In our previous paper[2] it was shown that the rate of the anodic PH oxidation on Pt is given by the following equation

$$i = nFC^{\beta}_{PH}C^{-2\beta}_{H+} \exp(\beta F\varphi/RT) \qquad (1)$$

Here, β is the activation coefficient of the Temkin isotherm which governs the adsorption-desorption steps involved, φ is any oxidation potential and the other figures have their usual meaning.

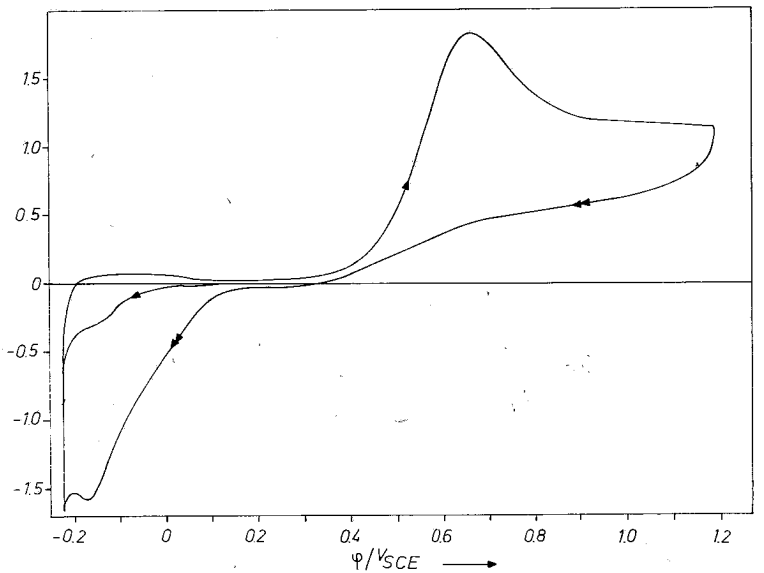

FIG. 2: *Current/potential diagram of 10^{-2} M PH in 1 M H_2SO_4 on Pt, v=100 mV s^{-1}, T=25°C, deaerated solution.*

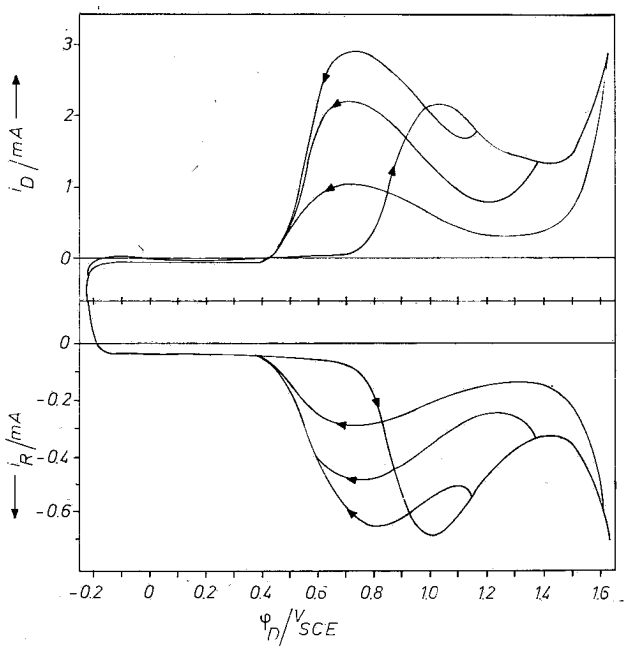

FIG. 3: *Disc-current/disc-potential diagram (above) and ring-current/disc-potential diagram (below) of 10^{-2}M DMH in 1 M H_2SO_4 on Pt, v_D=100 mVs^{-1}, φ_R=-75mV_{SCE}, f=35,8 Hz, T=25°C, deaerated solution.*

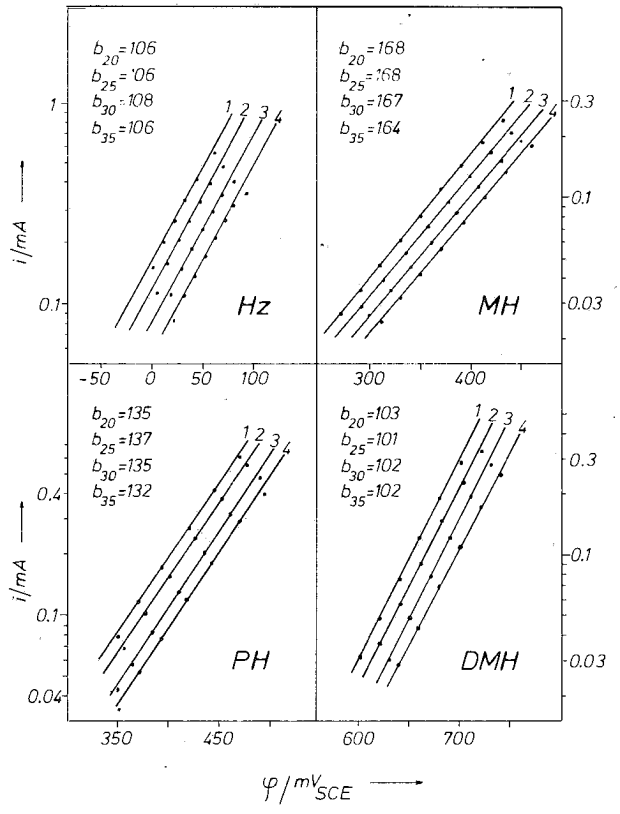

FIG. 4: *Tafel lines of the different hydrazine derivates (5.10^{-3}M) in 1 M H_2SO_4 on Pt, 1,35°C; 2,30°C; 3,25°C; 4,20°C.*
(b denotes slope in mV per 10 current units.)

With $\varphi = \varphi_o + \eta$, where φ_o is the rest potential and η the overpotential, and with $F\varphi_o = -\Delta G_o^{\neq}$ (the rate determining process is a 1-electron step) the following equation is easily derived.

$$i = nFC^{\beta}_{PH}C^{-2\beta}_{H+}\exp(\beta\Delta S/R)\exp(-\beta\Delta H^{\neq}_o/RT)\exp(\beta F\eta/RT) \qquad (2)$$

Therefore

$$\frac{\partial \ln i}{\partial(1/T)} = \frac{\beta F}{R}\eta - \frac{\beta\,\Delta H^{=}_o}{R} + \beta\frac{\partial \ln C_{PH}}{\partial(1/T)} - 2\beta\frac{\partial \ln C_{H+}}{\partial(1/T)} + \frac{\beta F}{RT}\frac{\partial\eta}{(1/T)} = \frac{\beta}{R}(F\eta - \Delta H^{=}_{o\ app}) \qquad (3)$$

In eq. (3) all temperature dependent terms are comprised in $\Delta H^{=}_{o\ app}$ which can easily be calculated for any potential chosen and then corrected to $\eta = 0$ as was proposed by Piersma and Gileadi.[6] These corrected $\Delta H^{\neq}_{o\ app}$ values, obtained from an average $\Delta H^{\neq}_o$ at an average potential, are given in Table I.

In the case of PH, $\Delta H^{\neq}_{o\ app.}$ evidently is given by

$$\Delta H^{\neq}_{o\ app} = \Delta H^{\neq}_{o\ true} - R\frac{\partial \ln C_{PH}}{\partial(1/T)} + 2R\frac{\partial \ln C_{H^+}}{\partial(1/T)} - \frac{F}{T}\frac{\partial \eta}{\partial(1/T)} \quad (4)$$

Similar equations can be derived for the other substituted hydrazines studied. Since the dependence of the concentration and the overpotential upon the temperature are unknown, the absolute values of $\Delta H^{=}_{o\ true}$ can not be calculated. The variation of the H^+-activity with temperature, however, is the same for all substances presented here, and the changes in the hydrazine concentrations and the overpotential can be assumed to be approximately the same for all compounds studied. Therefore, we believe that the difference between the apparent energy of activation of any of the hydrazine derivates and that of hydrazine itself is mainly due to a change in the true energy of activation and we define

$$\delta\Delta H^{\neq}_{o\ true} = \Delta H^{\neq}_{o\ app,\ derivate} - \Delta H^{\neq}_{o\ app,\ hydrazine} \quad (5)$$

These $\delta\Delta H^{\neq}_{o}$-values are also given in Table I and further considered in the discussion.

TABLE I: Measured peak potentials E_p and $\delta\Delta H^{\neq}_{o}$-values for the anodic oxidation of hydrazine and some of its derivates on Pt in 1.0 M sulfuric acid solution. T = 25°C.

substance	E_p (V_{SCE})	$\Delta H^{\neq}_{o\ app}$ (Kcal/mole)	$\delta\Delta H^{\neq}_{o}$ (Kcal/mole)	μ (D) after ref. 21
H_2NNH_2	0,22	26,4	0	1,9
CH_3NHNH_2	0,65	30,9	4,5	1,69
$C_6H_5NHNH_2$	0,68	31,15	4,75	1,76
$(CH_3)_2\ NNH_2$	0,81	33,0	6,6	1,36

Discussion

Let us first consider, as it was postulated in the literature, that within the oxidation of hydrazine an intermediate radical N_2H_3 |• appears in alkaline[7,8] and its protonated form $N_2H_4^+$ |• in acid solutions.[1] In the case of hydrazine derivates a corresponding radical, adsorbed at the electrode surface, must be assumed to appear before the rate determining step. Since the oxidation kinetics is determined by a one-electron step and according to the mechanism proposed[2,3,4], this adsorbed intermediate can be characterized as

$$\begin{matrix} R \\ N\,NH\ldots Pt \\ R \end{matrix}$$

where R stands for CH_3-, C_6H_5- or H-.

In the cases of PH and DMH the substituents stabilize the reducible intermediate so that the corresponding reduction peak can easily be found. With one methyl-group attached the intermediate is rather unstable, already, and in the case of hydrazine itself no indication of a reduction peak can be found. Furthermore, it can be concluded that the abstraction of the first hydrogen atom

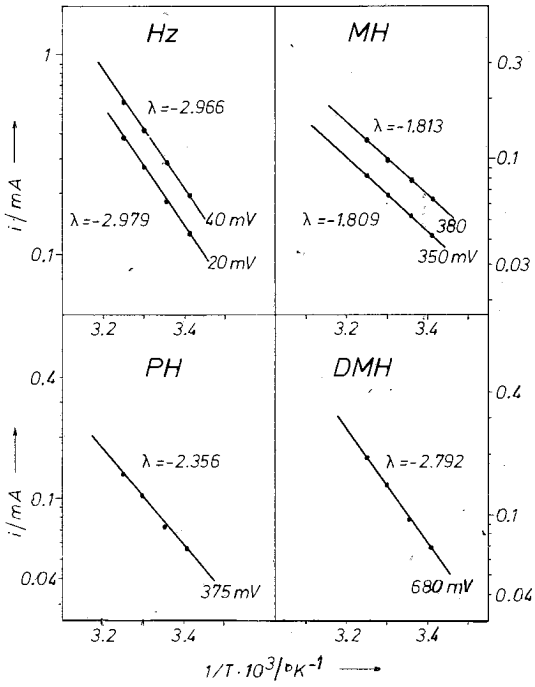

FIG. 5: *Arrhenius plots for the different hydrazine derivates at constant oxidation potentials. λ is the slope of the lines.*

from the hydrazine itself and from its derivates is a reversible process. Since the N-N bond is not split off within the anodic oxidation of hydrazine,[9,10] the irreversibility of the overall process is probably related to the change from the N-N single bond to a double bond structure. Hence, the influence of the substituents on the mechanism can be understood as a hindrace on this change and on the other hand as a stabilization of the reducible intermediate which then becomes detectable.

The effect of the substituents on the oxidation potential can be seen from Fig. 1. All substituted hydrazines have much higher oxidation potentials than hydrazine itself and the mono-substituted species are more readily oxidized than the di-substituted. Taking the peak potential E_p as a measure, we observe a potential shift of about 400 mV between hydrazine and its mono-methyl and mono-phenyl derivates and a further 200mV difference between the mono-and the di-methylsubstituted molecules.

To give a first global explanation these potential shifts could be assumed to be mainly attributed to the steric hindrance of the reaction by the substituents. Hydrazine itself is a symmetrical molecule and any of its four hydrogen atoms can be the first to be oxidized. The hydrazine derivates, however, are asymmetrical and the hydrogen abstraction must be assumed to occur at the non substituted side of the molecule.

But a closer look shows that the explanation of the potential shifts by steric effects is too simple because of the following reasons:

(1) Hydrazine itself is protonized in an acid solution ($H_2NN^+H_3$) and the positive charge attached to one of the two nitrogen atoms results in an

"electrostatical" hindrance on a positively charged electrode. Hence, the abstraction of the first hydrogen atom must be assumed to occur at the nonprotonized side of the molecule. This assumption is supported by the fact that the neutral hydrazine molecule in an alkaline solution is much more readily oxidized than the protonized form in acid electrolytes.[1,7,8] Consequently, hydrazine itself behaves in an acid electrolyte unsymmetrically to some extent.

(2) In the case of MH the inductive effect of the CH_3-group induces a (δ-)-charge in the hydrazine group and in the case of PH the electron withdrawing phenyl-group induces a (δ+)-charge. Therefore, it must be assumed to some extent that under the influence of the electric field in front of the electrode these molecules are directed towards the electrode in a different manner: the MH with its unsubstituted side towards the electrode, the PH with its phenyl-group towards the electrode, as illustrated in Fig. 6.

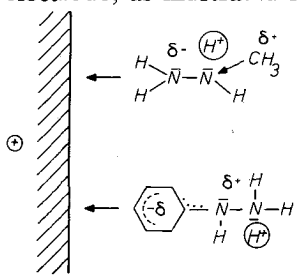

FIG. 6

But as can be seen from Tab. I, the peak potentials and the $\delta\Delta H_\delta^{\neq}$ -values of PH and MH do not show a significant difference. This idicates that a steric hindrance cannot be the main explanation for the change of the oxidation potentials.

(3) Finally a look to the current potentials diagrams (cf. Fig 1 and refs. 2-4) shows the hydrogen peaks to be suppressed even on a freshly activated electrode. Therefore, a preceeding adsorption of the hydrazines on the platinum surface has to be assumed, i.e.

$$[R_2N^+HNH_2 \rightleftarrows R_2N\,N^+H_3] \rightleftarrows R_2N\,NH_{2ads} + H^+ \qquad (6)$$

Such a step is plausible[11,12] regarding the dipol moments given in Tab I and was postulated already by Harrison and Khan.[1] Reaction (6) is a fast equilibrium process which does not interfere with the kinetics of the oxidation reaction and has nothing to do with the rate determining desorption step.[2-4]

Since the preceeding adsorption of the hydrazines occurs, a steric hindrance can only play a minor role in the explanation of the potential shifts caused by the substituents. In fact, the oxidation potential is determined by eq. (7)[1-4]

$$RNH\,NH_2 \ldots Pt \rightleftarrows R\,NH\,NH \ldots Pt + H^+ + e^- \qquad (7)$$

As can be seen from eq. (7), the rate of the intermediate formation is determined either by the abstraction of the first hydrogen atom or by the transfer of the first electron. In the case of the methyl-derivates, the strength of the hydrogen bonds is increased by the positive inductive effect and, therefore, for the hydrogen abstraction a higher energy is necessary. This fact also explains the difference between MH and DMH. In the case of PH, however, the electronic effect of the phenyl-group reduces the electron density of the (N - N) -group which results in a weakening of the hydrogen bonds. But because of the induced (δ +) -charge the electron transfer is hindered. Therefore, the introduction of a phenyl- or a methyl-group result in a slowing down of the reaction.

Furthermore, it is to be noticed that the value of the ratio

$$\frac{i_p\ (PH)}{i_p\ (MH)} = 0.72$$ is lower than the expected one

$$\frac{i_p\ (PH)}{i_p\ (MH)} = \sqrt{\frac{\alpha(PH).D\ (PH)}{\alpha(MH).D\ (MH)}} = 0.94$$

because of the lower active surface area caused by the flat adsorption of the ring structure[11,13-15] of the phenyl-group of PH or its reaction products, respectively. In the case of PH, however, a higher surface coverage than for MH is to be expected, since ∂ is a function of the dipol moment[11,12] and PH possesses greater μ-value than MH as Tab. I shows. Finally, the intermediate phenyldiimide is more stable than the corresponding methyldiimide which results in a greater selfinhibition in the case of the PH-oxidation.

The merely qualitative interpretation of the effects of the substituents on the oxidation potential given above can be represented in a semi-empirical way by regarding the influence of the $\delta\Delta H^{\neq}_o$ - values on the oxidation rate. In Fig. 7, the peak potentials E_p are plotted against $\delta\Delta H^{\neq}_o$. The result is a straight line which was also established in a similar way in some polarographic studies[16,17,18,19] plotting $E_{1/2}$ against the heat of activation or the Hammet-Taft-parameters, respectively. Since the peak potentials are mainly determined by the logarithm of the heterogeneous rate constants,[2] Fig. 7 seems to indicate that the well known linear relationship between the logarithm of the rate of the reaction and the heat of activation holds for the case of the electrochemical oxidation of hydrazine.

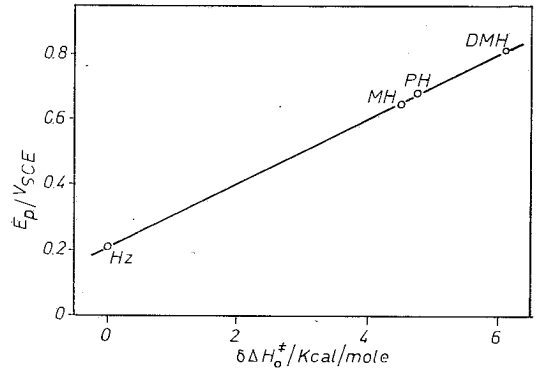

FIG. 7: *Peak potentials E_p against the change of enthalpy $\delta\Delta H^{\neq}_o$.*

This linear heat of activation relationship can be proved by plotting the oxidation currents of the different derivates extrapolated from the measured Tafel lines for a constant potential against $\delta\Delta H^{\neq}_o$. This was done in Fig. 8 for $\varphi = 300$ mV_{SCE} and 25°C.

From eq. (2) the following relation can be derived, where all terms not depending on the derivates are comprised in the constant K.

$$\ln i = K + \beta \ln C_{PH} + \beta\Delta S^{\neq}_o/R - \beta/RT\,(\delta\Delta H^{\neq}_o - F\eta) \qquad (8)$$

Hence, with the assumption that the concentrations and $\Delta S^{=}{}_{o}$ are only of low influence, a slope of - β/RT should be expected in fig. 8, as it is realized. The deviations from the exact linearity in fig. 8 are due to the differences in β for the different derivates as well as to the uncertainty in the rest potentials.[2,3,4]

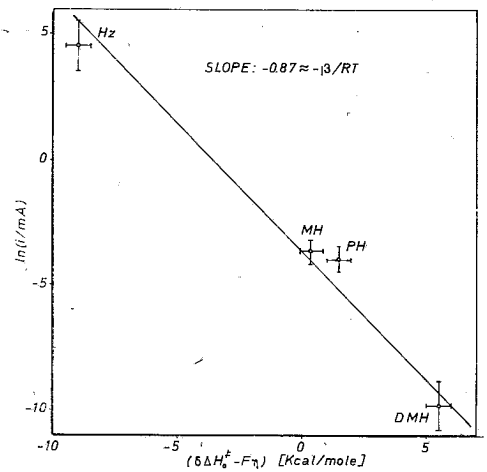

FIG. 8: *Oxidation rates of the different hydrazine derivates at φ = 300 mV$_{SCE}$ against the change of enthalpy $\delta\Delta H^{\neq}{}_{o}$*

Fig. 8 clearly indicates that the linear heat of activation relationship is applicable in the case of the anodic oxidation of hydrazines. Consequently, the reaction, which determines the oxidation potential, is the same for all the hydrazines considered and is given by eq. (7). If this condition was not fulfilled, no linear relationship could be expected.[20]

Περίληψη

Ἐπίδραση τῶν ὑποκατάστατων στὸ μηχανισμὸ καὶ στὴν ταχύτητα τῆς ἀνοδικῆς ὀξειδώσεως τῆς ὑδραζίνης σὲ ὄξινα διαλύματα

Μελετᾶται ἡ ἐπίδραση τῶν μεθυλο- καὶ φαινυλο-ομάδων στὸ μηχανισμὸ καὶ στὴν ταχύτητα ὀξειδώσεως τῆς ὑδραζίνης στὸ λευκόχρυσο σὲ ὄξινα μὲ θειικὸ ὀξὺ διαλύματα. Παρέχονται τὰ διαγράμματα ἐντάσεως-τάσεως καὶ οἱ κλίσεις Tafel σὲ διάφορες θερμοκρασίες τῶν οὐσιῶν ὑδραζίνης, μεθυλυδραζίνης, διμεθυλυδραζίνης καὶ φαινυλυδραζίνης. Ἀπὸ τὰ διαγράμματα log i - 1/T ὑπολογίζονται οἱ ἐνέργειες ἐνεργοποιήσεως τῶν ἀντίστοιχων ἠλεκτροχημικῶν δράσεων καὶ λαμβάνονται οἱ διαφορὲς $\delta\Delta H_o$ μεταξὺ τῶν παραγώγων καὶ τῆς μητρικῆς ἐνώσεως.

Ἡ ἐξάρτηση τοῦ E_p καὶ τοῦ log i — σὲ σταθερὸ δυναμικὸ — ἀπὸ τὴ $\delta\Delta H_o$ ἀκολουθεῖ τὴ γνωστὴ γραμμικὴ ἐξίσωση Hammet πράγμα ποὺ σημαίνει ὅτι ἡ ἀντίδραση ποὺ καθορίζει τὸ δυναμικὸ ὀξειδώσεως ὅλων τῶν παραπάνω οὐσιῶν εἶναι ἡ ἴδια καὶ παρέχεται ἀπὸ τὴν ἐξίσωση (7).

References and Notes

1 Harrison J.A. and Khan Z.A.: *J. Electroanal. Chem.*, **28**, 131 (1974)
2 Karabinas P. and Heitbaum J.: *J. Electroanal. Chem.*, **65**, 685 (1975)
3 Karabinas P. and Heitbaum J.: *J. Electroanal. Chem.*, **76**, 235 (1977)
4 Karabinas P. and Heitbaum J.: *J. Electroanal. Chem.*, *76*, 247 (1977)
5 Hills G.J. and Ives D.J.G. in "Reference Electrode" p. 161 (Edited by Ives D.J.G., Janz G.J.) Academic Press, N.Y. (1961)
6 Piersma B.J. and Gileadi E. in "Modern Aspects of Electrochemistry" (Edited by Bockris J.O'M.) Vol. 4. pp145-7 Butterworths, London, 1966.
7 Harrison J.A. and Khan Z.A.: *J. Electroanal. Chem.*, **26**, 1 (1970)
8 Heitbaum J. and Vielstich W.: *Electrochim. Acta*, **18**, 501 (1973)
9 Bruckenstein S. and Comeau J.: *Disc. Faraday Soc.*, **56**, 285 (1974)
10 Arnolds K. Heitbaum J. and Vielstich W.: *Z. Naturforschung*, **29** a, 359 (1974)
11 Bockris J. O'M., Gileadi E. and Müller K.: *Electrochim. Acta* **12**, 1301 (1967)
12 Devanathan M.A.V. and Tilak B.V.K.S.R.A.: *Chem. Rev.*, **65**, 635 (1965)
13 Conway B.E. and Barradas R.G.: *Electrochim. Acta*, **5**, 319 and 349 (1961)
14 Conway B.E., Barradas R.G. and Zavidzki T.: *J. Phys. Chem.*, **62**, 676 (1958)
15 Frumkin A.N. and Damaskin B.B. in "Modern Aspects of Electrochemistry", Vol 3,p 163, (Edited by Bockris J.O'M. and Conway B.E. Butterworths, London 1964
16 Zuman P.: *"Substituent Effects in Organic Polarography"*, Plenum Press, N.Y. 1967
17 Brockmann R.W. and Pearson D.E.: *J. Am. Chem. Soc.*, **74**, 4128 (1952)
18 Gergely E. and Iredale T.: *J. Chem. Soc.*, 3226 (1953)
19 Lawrence A.R. and Ferguson L.N.: *Nature*, **183**, 1469 (1959)
20 Ingold C.K.: "*Structure and Mechanism in Organic Chemistry*" 2nd Ed. Cornell Univ. Press, Ithaca and London 1969
21 McClellan A.L.: *"Tables of Experimental Dipole Moments"*, Freeman W. & Co, San Francisco 1963
22 Schmickler W.: *Electrochim. Acta*, **21**, 161 (1976)

Chimika Chronika, New Series. 7, 189-196 (1978)

1,3-DIPOLAR CYCLOADDITION OF NITRILE OXIDES TO TRIMETHYLSILYL ENOL ETHERS. PREPARATION OF 5-TRIMETHYLSILYLOXY-Δ^2-ISOXAZOLINES.

D.N. NICOLAIDES and A.G. CATSAOUNIS
Laboratory of Organic Chemistry, Univ. of Thessaloniki, Thessaloniki (Greece)
(Received December 1, 1977)

Summary

1,3-Cycloaddition of benzonitrile oxide and 2,6-dichloro-benzonitrile oxide with trimethylsilyl enol ethers of mono-ketones and β-diketones and also with enol benzoates of benzoylacetone was studied. The reaction with silyl enol ethers gave regioselectively Δ^2-isoxazolines, which was not always possible to be isolated, while with enol benzoates gave directly the corresponding isoxazoles. The structure of the isolated new cycloaddition products is confirmed by their spectral data (NMR, MS).

Key words: 5-Trimethylsilyloxy-Δ^2-isoxazolines, isoxazoles, preparation, regioselective cycloaddition, NMR, MS spectra.

Introduction

The 1,3-dipolar cycloaddition of nitrile oxides to alkenes is the most general method of preparation of Δ^2-isoxazolines and represents a convenient route to isoxazoles[1]. Generally isoxazolines are stable compounds, but it has been shown that some substituents can be easily eliminated giving rise to the more stable aromatic isoxazole ring. Quilico and Speroni[2] found that benzonitrile oxide *(5a)* reacts with β-diketones, only in the presence of a base, forming isoxazoles of structure *8*. They suggested that the reaction involves a 1,3-dipolar cycloaddition of the nitrile oxide to the enol form of the β-diketone *6* (Y = H), with subsequent dehydration of the resulting Δ^2-isoxazoline-5-ol *7* (Y = H), which can not be isolated. D'Alcontres and Grünanger[3] obtained 3-phenylisoxazole by heating 3-phenyl-5-acetoxy-Δ^2-isoxazoline with methanolic hydrogen chloride and assumed that it was formed by dehydration of the intermediate alcohol, which was

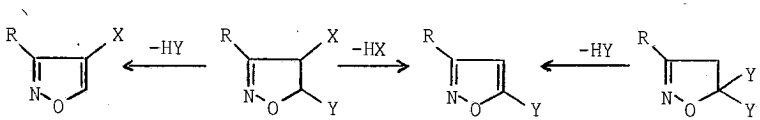

2 1 3 4

not isolated. Many other 5-acetoxy-Δ^2-isoxazolines are converted to the corresponding isoxazoles, under similar conditions[4]. It has also been noted that isoxazolines of structure *1*, with X = Cl[5], NO_2[6] or Y = Cl[7,8], Br[7], amine[8-12], NO_2[13], N_3[14] readily eliminate HY or HX to give isoxazoles *2* and *3* respectively. Isoxazoles *3* have also been obtained from isoxazolines *4*, with Y = OR^{15}, SR^{16}, amine[17], by elimination of YH.

In spite of the extensive literature on 1,3-dipolar cycloadditions of nitrile oxides with a wide variety of olefinic dipolarophiles, reactions of this type involving silyl enol ethers have not been reported. In this work we studied the 1,3-cycloaddition reactions of nitrile oxides *5(a,b)* with trimethylsilyl enol ethers *6(a,b), 9* and *10* as well as with enol benzoates *6(c,d)* in order to prepare trimethylsilyloxy- and benzoyloxy- Δ^2-isoxazolines. The structure of the cycloaddition products was also studied on the basis of their spectral data (NMR, MS), in order to investigate the orientation effect of the silyloxy group in the examined regioselective cycloaddition reactions.

Results and discussion

Treatment of trimethylsilyl enol ethers *6(a,b)* with benzonitrile oxide *(5a),* prepared *in situ* from benzhydroximic acid chloride (Method A), gave directly the known isoxazoles *8a, 8b* in 29% and 26% yield respectively (Table I). Compounds *8a, 8b* were identical to those prepared, under similar conditions, from benzonitrile oxide and the sodium salt of acetylacetone and benzoylacetone respectively. Treatment of enol benzoates *6c* (E-isomer) and *6d* (Z-isomer) with *5a,* under the same conditions, gave again directly isoxazole *8b* in 8% and 5% yield respectively. By contrast to the previous described reactions, when the silyl enol ether *6a* and freshly prepared 2,6-dichloro-benzonitrilr oxide *(5b)* were heated under reflux in ether (Method B), gave both the 5-silyloxy-Δ^2-isoxazoline *7a* and the corresponding isoxazole *8c.* Separation of the reaction mixture by column chromatography (on silica gel) gave fractions containing mainly the isoxazoline *7a* and gradually increased amounts of the isoxazole *8c.* The NMR spectra (in CCl_4) of these eluted mixtures showed, besides the peaks of *8c* (Table I), peaks for *7a* at δ = 7.34 (br.s, 3H), 4.69 (s, 1H), 2.10 (s, 3H), 1.62 (s, 3H), and 0.20 ppm (s, 9H, $SiMe_3$) and also showed that compound *7a* was slowly converting to *8c.* Isoxazoline *7a* was completely converted to isoxazole *8c* during the procedure for further separation of the mixture by preparative t.l.c. (silica gel, ether: petroleum ether 3:7, extraction with chloroform). The total yield in *8c* was 30%. Similarly, from the reaction between *5b* and *6b* isoxazoline *7b* was separated as a mixture along with the isoxazole *8d* and was detected in the NMR spectrum (in CCl_4) showing peaks at δ = 7.18-8.03 (m, 8H), 5.72 (s, 1H), 1.48 (s, 3H) and 0.28 ppm (s, 9H). On further purification by preparative t.l.c. compound *7b* was also completely converted to *8d.* Compound *8d* was directly obtained in 13% yield from the reaction between *5b* and the enol benzoate *6c.*

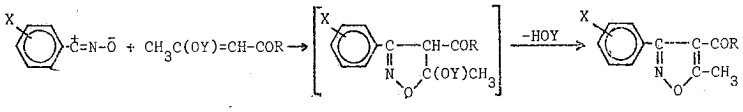

5 6 7 8

5a:X=H
b:X=2,6-Di-Cl

6a:R=CH_3, Y=$Si(CH_3)_3$
b:R=C_6H_5, Y=$Si(CH_3)_3$
c:R=C_6H_5, Y=C_6H_5CO (-E)
d:R=C_6H_5, Y=C_6H_5CO (-Z)

7a:X=2,6-Di-Cl, R=CH_3 Y=$Si(Ch_3)_3$
b:X=2,6-Di-Cl, R=C_6H_5 Y=$Si(cH_3)_3$

8a:X=H, R=CH_3
b:X=H, R=C_6H_5
c:X=2,6-Di-Cl, R=CH_3
d:X=2,6-Di-Cl, R=C_6H_5

Treatment of the silyl enol ethers *9* and *10* with benzonitrile oxide (*5a*), according to method A, afforded the isoxazolines *11a* and *12a* respectively. The

TABLE I. *Isoxazoles 8(a-d) prepared from 5(a,b) and 6(a-d) via the corresponding Δ^2 - isoxazolines 7.*

Product	5 (used mmol)[a]	6 (used mmol)	Method	Reaction time (h)	Yield (%)[b]	M.p./Recryst. solvent	Molecular Formula	Calculated/Found %C	%H	%N	^{1}H-NMR (CCl_4) δ(ppm)
8a	5a (42)	6a (38)	A	24	29	58-59°,[c] P. ether	$C_{12}H_{11}NO_2$	71.62 71.85	5.51 5.48	6.96 7.09	7.48 (br.s, 5H), 2.65 (s, 3H), 1.98 (s, 3H, $COCH_3$)
8b	5a (19)	6b (10)	A	24	26	115-116°,[d] Ether	$C_{17}H_{13}NO_2$	77.55 77.87	4.98 5.04	5.32 5.77	7.12 - 7.75 (m, 10H), 2.48 (s, 3H)
8b	5a (5.3)	6d (2.8)	A	12	5						
8c	5b (18.6)	6a (15.7)	B	28	30	73-74°, P. ether	$C_{12}H_9Cl_2NO_2$	53.35 53.14	3.36 3.40	5.19 4.95	7.45 (br.s, 3H), 2.78 (s, 3H): 1.92 (s, 3H, $COCH_3$)
8d	5b (15)	6b (13)	B	24	10	143-144°, CCl_4	$C_{17}H_{11}Cl_2NO_2$	61.46 60.95	3.34 3.35	4.22 4.25	7.10 - 7.70 (m, 8H), 2.63 (s, 3H)

a: In reactions of Method A the mmol of benzhydroximic acid chloride used are given.
b: Total yield based on dipolarophile 6 used.
c: Lit.[2], m.p. 60°.
d: Lit.[2], m.p. 115-116°.

TABLE II. *Δ^2 - Isoxazolines 11(a,b), 12(a,b) prepared from 5(a,b) and Trimethylsilyl Enol Ethers 9, 10.*

Product	5 (used mmol)[a]	Dipolarophile (used mmol)	Method Reaction time (h)	M.p. Recryst. solvent	Molecular Formula Yield (%)[b]	Calculated/Found %C	%H	%N	^{1}H-NMR (CCl_4) δ (ppm)
11a	5a	9	A	81-82°	$C_{16}H_{23}NO_2Si$	66.39	8.01	4.84	7.27-7.82 (m, 5H), 3.07 (t, 1H, J=8 Hz),
	(10)	(5.9)	10	P. ether	14	66.40	7.99	4.83	1.05-2.50 (m, 8H), 0.12 (s, 9H, $SiMe_3$)
11b	5b	9	B	84-85°	$C_{16}H_{21}Cl_2NO_2Si$	53.62	5.91	3.91	7.33 (br.s, 3H), 3.25 (t, 1H, J=8 Hz),
	(8)	(5.9)	24	P. ether	18	53.67	5.89	4.05	1.13-2.50 (m, 8H), 0.15 (s, 9H, $SiMe_3$)
12a	5a	10	A	80-82°	$C_{18}H_{21}NO_2Si$	69.41	6.80	4.50	7.18-7.80 (m, 10H) 3.50 (d, 1H, J=17 Hz),
	(19)	(12)	24	CCl_4	59 →	70.03	6.76	4.51	3.30 (d,1H, J=17 Hz), 0.11 (s, 9H, $SiMe_3$)
12b	5b	10	B		$C_{18}H_{19}Cl_2NO_2Si$				7.13-7.65 (m,8H), 3.43 (d, 1H, J=17.5 Hz),
	(5.3)	(2.7)	45		45				3.33 (d, 1H, J=17.5 Hz) 0.13 (s, 9H, $SiMe_3$)

a: In reactions of Method A the mmol of benzhydroximic acid chloride used are given.
b: Based on dipolarophile 9 or 10 used.

same dipolarophiles gave with *5b* (method B), the corresponding isoxazolines *11b* and *12b* (Table II). Compounds *11(a,b)* and *12(a,b)* were isolated from the reaction mixtures by column chromatography and their NMR spectra (Table II) are in agreement to the given structures. Isoxazolines *11(a,b)* and *12a* were further purified and stored for a long time without decomposition, while compound *12b* turned quickly to the corresponding isoxazole as it is indicated by its NMR spectrum.

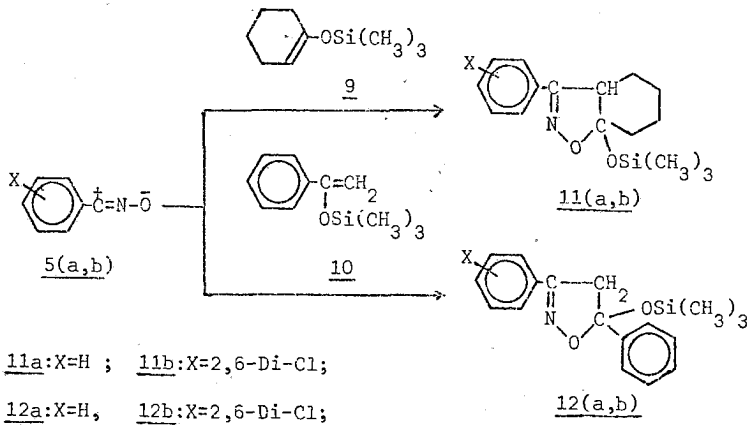

11a:X=H ; 11b:X=2,6-Di-Cl;

12a:X=H, 12b:X=2,6-Di-Cl;

Although the stereochemistry of the intermediate Δ^2-isoxazolines *7* is not proven, these compounds can be considered to result from a stereospecific *syn* addition, in conformity with the stereochemical course of all 1,3-dipolar cycloaddition reactions[18]. The silyl enol ethers *6a, 6b,* used in the reactions, were mixtures of *cis-trans* isomers, since reported attempts to separate them were unsuccessful, because equilibrium is established readily between the two isomers[19]. The isolated isoxazolines *7a* and *7b* were individual isomers and not mixtures of the possible stereoisomers, as it is indicated from their NMR spectra and especially from the unique singlet for C_4-proton, because the chemical shifts of this proton in similar diastereomers are different[8,20]. Concerning the stereochemistry of compounds *7* it might be argued that the facile elimination of H-OY from their molecule is in better agreement with the *anti* position of C_4-H and C_5-OY, as in the case of 5-azido-Δ^2-isoxazolines[14]. This argument, however, should be used with much reservation, since *syn* elimination is also a possible, although less favourable, pathway[14,21]. In this case an *anti* elimination can also be assumed, considering an interconversion in the structure of the stereoisomers.

With respect to the regiochemical course of the cycloaddition, the finally obtained isoxazoles *8(a-d)* demonstrate that this follows a regioselective process, with exclusive formation of the suggested orientational isomers *7*. The 1,3-cycloaddition of nitrile oxides *5(a,b)* to dipolarophiles *9, 10* is also regioselective, leading exclusively to the isoxazolines *11(a,b), 12(a,b).* The proposed structures were established by their NMR spectra, since the recorded chemical shifts for C_4-H of compounds *11(a,b)* and *12(a,b)* (Table II) are in good agreement with those reported for similar 5-pyrrolidino-[9] and 5-azido-Δ^2-isoxazolines[14]. The structure of isoxazolines *12(a,b)* was further confirmed through their conversion to the corresponding isoxazoles[22].

Although the recorded chemical shifts for the C_5-methyl protons in the NMR spectra of the new compounds *8c, 8d* are in good agreement with the proposed structure, being very similar to those of the known compounds *8a, 8b* and to those of other 5-methyl-isoxazoles[23], it must be pointed out that similar chemical shifts have also been reported for the C_4-methyl protons of some 4-methyl-5-benzoyl-isoxazoles[14]. Another strong evidence in favour of the suggested structure for isoxazoles *8c, 8d* is the fact that in the recorded mass spectra of compounds *8(a-d)* the abundant ion m/e 43 (CH_3-C$\equiv$O) and the less abundant ion (M-42) (loss of ketene), characteristic for 5-methyl-isoxazoles[24], were observed (Table III).

TABLE III: *Mass spectral data of isoxazoles 8(a-d) and isoxazolines 11(a,b), 12a. Mass numbers and relative intensities (values in parenthesis).*

Compound	Mass numbers (m/e) and relative intensities
8a	201 (100), 186 (21), 159 (56, M-42), 144 (92), 117 (12), 116 (10, M-85), 105 (6), 77 (24), 43 (32).
8b	263 (90), 248 (5), 235 (11), 234 (13), 221 (10, M-42), 220 (9), 193 (8), 144 (15), 105 (100), 77 (45), 43 (17).
8c	269 (0.1), 254 (0.2), 234 (100, M-Cl), 227 (1.5, M-42), 219 (4), 217 (10), 214 (20), 212 (31), 192 (4, 234-42), 184 (6, M-85), 149 (2, 234-85), 43 (51).
8d	331 (2.5), 296 (100, M-Cl), 289 (1.5, M-42), 254 (16, 296-42), 105 (67), 77 (63), 43 (50).
11a	289 (35), 274 (29, M-15), 246 (47, 274-C_2H_4), 199 (38, M-HOSiMe_3), 178 (19), 172 (24), 171 (24), 170 (42, M-C_6H_5CNO), 155 (19), 143 (33), 130 (44), 77 (37), 75 (100), 73 (50).
11b	357 (23), 342 (32, M-15), 314 (35, 342-C_2H_4), 267 (15, M-HOSiMe_3), 242 (11), 241 (10), 240 (18), 239 (14), 232 (10, 267-Cl), 226 (10), 213 (8), 211 (9), 206 (10), 204 (29), 200 (12), 198 (29), 170 (63), 75 (100), 73 (97).
12a	311 (21), 296 (13, M-15), 221 (92, M-HOSiMe_3), 193 (15), 165 (7), 144 (27, 221-C_6H_5), 117 (15), 116 (8), 105 (100), 89 (14), 77 (74), 75 (98), 73 (9).

Although in the case of isoxazoles *8a, 8c* these fragments can also be directly formed from the acyl group, present in their molecule, the moderate ion (M-85), observed only in their mass spectra can be attributed to a fragmentation pathway, involving elimination of both, the $CH_3CO^{\cdot}$ and the ketene from the molecular ion, with participation in this process of the C_5-methyl group. The molecular ions of compounds *8c, 8d* were found in very low abundance, while ions (M-Cl) appeared as the base peaks in their mass spectra. Compounds *8a, 8c* follow generally a similar fragmentation pattern, especially if we consider for *8c* the further fragmentation of the (M-Cl) abundant ion. The same behaviour is also observed in the other pair of analogous isoxazoles *8b, 8d*. In the mass spectra of the 5-trimethyl-silyloxy-Δ^2-isoxazolines *11a, 11b, 12a* the abundant ions (M-15), m/e 75 (H-O= $SiMe_2$) and m/e 73 ($SiMe_3$), characteristic for the fragmentation of the trimethylsilyloxy

group[25,26], were observed (Table III). In addition to these, the general feature in the fragmentation process of the studied isoxazolines is the loss of the H-OSiMe$_3$ group from the molecular ion with formation of abundant isoxazole ions. These followed further fragmentation, involving cleavage of the isoxazole ring and the substituents, in agreement with reported fragmentation mechanisms for similar compounds[27].

From the reactions discussed above it is evident that the trialkyl-silyloxy group, like the amine group in enamines[8-12], has a pronounced directional effect on cycloadditions. This property can be utilized for preparative work, since trialkylsilyl enol ethers can be easily prepared from carbonyl compounds in high yield, by several methods[19,26,28]

Experimental

M.p's are given without correction and were determined with a Kofler hot-stage apparatus. NMR spectra were obtained in carbon tetrachloride with a Varian A-60A spectrometer with tetramethylsilane as internal standard. The mass spectra were obtained with a Hitachi Perkin-Elmer RMU-6L mass spectrometer; the ionization energy was maintained at 70 eV. Earlier reported procedures were used for the preparation of the benzhydroximic acid chloride[29], 2,6-dichloro-benzonitrile oxide[30], trimethylsilyl enol ethers *6(a,b)*[28], enol benzoates *6(c,d)*[31] and trimethylsilyl enol ethers *9, 10*[26].

General procedures for the cycloaddition reactions of nitrile oxides 5a *(Method A) and* 5b *(Method B) with dipolarophiles* 6(a-d), 9 and 10.

Method A.

In this method the benzonitrile oxide was prepared *in situ* from benzhydroximic acid chloride. To a stirred and ice-cooled ethereal solution of benzhydroximic acid chloride and dipolarophile (for every 10 mmol of benzhydroximic acid chloride 50 ml of ether were used) a stoichiometric amount of triethylamine in ether (10 mmol of triethylamine in 20 ml of ether) was added over one hour period. The mixture was stirred for further 2 h under cooling and then for ~20 h at room temperature (see Tables I, II). The triethylamine hydrochloride was filtered off, the filtrate was partly concentrated under reduced pressure and petroleum ether was added to precipitate part of the produced 3,4-diphenyl-furoxan. The mixture was cooled, the furoxan was filtered off and the concentrated filtrate was further separated by column chromatography on silica gel, eluted with light petroleum containing increasing amounts of ether.

Method B.

An ethereal solution of freshly prepared 2,6-dichloro-benzonitrile oxide (*5b*) and the dipolarophile (for every 10 mmol of *5b* 30 ml of ether were used) was heated under reflux for several hours (see Tables I, II). The reaction was monitored by t.l.c. The solution was partly concentrated under reduced pressure, petroleum ether was added to precipitate the produced furoxan and the mixture was then worked up like in method A.

In all reactions of Table I the produced furoxans were eluted first from the column, followed by the cycloaddition products, while in the reactions of Table II the cycloaddition products were eluted first and in some cases as mixtures with furoxan. The content of each fraction was checked by NMR.

Περίληψη

1,3-Διπολική κυκλοπροσθήκη νιτριλοξειδίων σὲ τριμεθυλοσιλυλο-ενολαιθέρες. Παρασκευὴ 5-τριμεθυλοσιλυλοξυ-Δ^2-ισοξαζολινῶν.

Μελετοῦνται ἀντιδράσεις 1,3-διπολικῆς κυκλοπροσθήκης τῶν νιτριλοξειδίων *5a, 5b* μὲ τοὺς τριμεθυλοσιλυλο-ενολαιθέρες β-δικετονῶν *6a, 6b* καὶ μονοκετονῶν *9, 10* ὅπως καὶ μὲ τοὺς βενζοϊκοὺς ἐστέρες τῆς ἐνολικῆς μορφῆς τῆς βενζοϋλακετόνης *6c, 6d.* Σὲ ὅλες τὶς περιπτώσεις παρατηρήθηκε στερεοεκλεκτική, μὲ καθορισμένο προσανατολισμὸ (regioselective) κυκλοπροσθήκη τοῦ νιτριλοξειδίου στὸν αἰθυλενικὸ διπλὸ δεσμὸ μὲ ἀποτέλεσμα τὸν ἀρχικὸ σχηματισμὸ τῶν Δ^2-ἰσοξαζολινῶν *7, 11, 12.* Ἀπὸ τὶς ἀντιδράσεις ποὺ ἀναφέρονται στὸν πίνακα I ἀπομονώθηκαν (μὲ χρωματογραφία στήλης) μόνο οἱ ἀσταθεῖς ἰσοξαζολίνες *7a, 7b* (ὅπως διαπιστώθηκε ἀπὸ τὴν μελέτη τῶν φασμάτων NMR τῶν κλασμάτων), οἱ ὁποῖες μετατράπηκαν ἀμέσως πρὸς τὰ ἀντίστοιχα ἰσοξαζόλια *8c, 8d,* ἐνῶ ἀπὸ ὅλες τὶς ἀντιδράσεις τοῦ πίνακα αὐτοῦ ἀπομονώθηκαν τὰ ἀντίστοιχα ἰσοξαζόλια *8.* Ἀντίθετα, ἀπομονώθηκαν καὶ μελετήθηκαν οἱ σταθερὲς ἰσοξαζολίνες *11a, 11b, 12a* τοῦ πίνακα II, ἐνῶ ἡ *12b* μετὰ τὴν ἀπομόνωσή της (φάσμα NMR) μετατράπηκε τελικὰ πρὸς ἰσοξαζόλιο στὴν προσπάθεια γιὰ τὸν παραπέρα καθαρισμό της μὲ χρωματογραφία λεπτῆς στιβάδας.

Ἡ δομὴ ποὺ προτείνεται γιὰ τὰ προϊόντα κυκλοπροσθήκης συμφωνεῖ μὲ τὰ φάσματα NMR τῶν ἰσοξαζολίων καὶ ἰσοξαζολινῶν ποὺ ἀπομονώθηκαν, ὅπως καὶ μὲ ὁρισμένες χαρακτηριστικὲς διασπάσεις ποὺ παρατηροῦνται στὰ φάσματα μάζης τῶν προϊόντων αὐτῶν.

Ἀπὸ τὴν ὅλη μελέτη τῶν ἀντιδράσεων τῶν τριμεθυλοσιλυλο-ενολαιθέρων, οἱ ὁποῖοι χρησιμοποιοῦνται γιὰ πρώτη φορὰ σὲ ἀντιδράσεις 1,3-διπολικῆς κυκλοπροσθήκης μὲ νιτριλοξείδια, προκύπτει ὅτι ἡ ὁμάδα $-OSi(CH_3)_3$ παρουσιάζει τὸ ἴδιο προσανατολιστικὸ ἀποτέλεσμα (regioselectivity) στὴν πορεία τῆς κυκλοπροσθήκης σὲ τριμεθυλοσιλυλο-ενολαιθέρες, ὅπως ἡ ἀμινικὴ ὁμάδα γιὰ τὶς ἐναμίνες.

References and Notes

1. Grundmann C. and Grünanger P.: *The Nitrile Oxides,* p.96, Springer-Verlag, Berlin (1971).
2. Quilico A. and Speroni G.: *Gazz. Chim. Ital.* **76**, 148 (1946).
3. D'Alcontres G. Stagno and Grünanger P.: *Gazz. Chim. Ital.,* **80**, 741 (1950).
4. Mukaiyama T. and Hoshino T.: *J. Am. Chem. Soc.:* **82**, 5339 (1960); Paul R. and Tchelitcheff S.: *Bull. Soc. Chim. Fr.* 2215 (1962); Just G. and Dahl K.: *Tetrahedron Lett.* 2441 (1966); Micetich R.G.: *Can. J. Chem.* **48**, 467 (1970).
5. Grünanger P. and Mangiapan S.: *Gazz. Chim. Ital.* **88**, 149 (1958); Finzi P. Vita and Arbasino M.: *Ann. Chim. (Rome)* **54**, 1165 (1964).
6. Grünanger P.: *Gazz. Chim. Ital.* **84**, 359 (1954).
7. Micetich R.G.: *Can. J. Chem.* **48**, 3753 (1970).
8. Bast K., Christl M., Huisgen R., Mack W. and Sustmann R: *Chem. Ber.* **106**, 3258 (1973).
9. Kuehne M.E., Weaver S.J. and Franz P.: *J. Org. Chem.* **29**, 1582 (1964).
10. Bianchetti G., Pocar D., Croce P. Dalla and Vigevani A.: *Chem. Ber.* **98**, 2715 (1965).
11. Stork G. and Mc Murry J.E.: *J. Am. Chem. Soc.* **89**, 5461 (1967).
12. Caramella P. and Cereda E.: *Synthesis* 433 (1971).
13. Shvekhgeimer G.A., Baranski A. and Grzegozek M.: *Synthesis* 612 (1976).
14. L'abbe G. and Mathys G.: *J. Org. Chem.* **39**, 1221 (1974).

15. Scarpati R. and Speroni G.: *Gazz. Chim. Ital.* **89**, 1511 (1959).
16. Scarpati R., Santamaria C. and Sica D.: *Gazz. Chim. Ital.* **93**, 1706 (1963).
17. Rajagopalan P. and Talaty C.N.: *Tetrahedron Lett.* 4537 (1966); Sasaki T. and Kojima A.: *J. Chem. Soc (C)* 476 (1970).
18. Huisgen R.: *Angew. Chem.* **75**, 742 (1963); *J. Org. Chem.* **33**, 2291 (1968).
19. Pinnavaia T.J., Collins W.T. and Howe J.J.: *J. Am. Chem. Soc.* **92**, 4544 (1970).
20. Sustmann R., Huisgen R. and Huber H.: *Chem. Ber.* **100**, 1802 (1967).
21. Sicher J.: *Angew. Chem.* **84**, 177 (1972); *Angew. Chem. Int. Ed. Engl.* **11**, 200 (1972).
22. Nicolaides D.N., Kanetakis M. and Litinas C.: to be published.
23. Micetich R.G.: *Can. J. Chem.* **48**, 2006 (1970); Padwa A., Chen E. and Ku A.: *J. Am. Chem. Soc.* **97**, 6484 (1975).
24. Ohashi M., Kamachi H., Kakisawa H., Tatematsu A., Yoshizumi H. and Nakata H.: *Tetrahedron Lett.* 379 (1968); Bowie H., Kallury R.K.M.R. and Cooks R.G.: *Aust. J. Chem.* **22**, 563 (1969).
25. Diekman J., Thomson J.B. and Djerassi C.: J. *Org. Chem.* **32**, 3904 (1967).
26. House H.O., Czuba L.J., Gall M. and Olmstead H.D.: *J. Org. Chem.* **34**, 2324 (1969).
27. Beam C.F., Dyer M.C.D., Schwarz R.A. and Hauser C.R.: *J. Org. Chem.* **35**, 1806 (1970).
28. West R.: *J. Am. Chem. Soc.* **80**, 3246 (1958); Kusnezowa T.K., Kuhlmann K. and Grindemann E.: *J. Organometal. Chem.* **47**, 53 (1973); Simchen G. and Kober W.: *Synthesis* 259 (1976); Torkelson S. and Ainsworth C.: *Synthesis* 722 (1976); Rasmussen J.K.: "O-Silylated Enolates-Versatile Intermediates for Organic Synthesis" *Synthesis* 91 (1977) and references cited therein.
29. Rajagopalan P., Advani B.G. and Talaty C.N. in Wiberg K.B.: *Organic Syntheses*, Vol. 49, p.71, Wiley, New York (1969).
30. Grundmann C. and Dean J.M.: *J. Org. Chem.* **30**, 2809 (1965).
31. Larkin J., Murray M.G., Nonhebel D.C. and Mitchell A.D.: *J. Chem. Soc. Perkin Trans. I*, 380 (1976).

Chimika Chronika, New Series, 7, 197-202 (1978)

SYNTHÉSE ET ÉTUDE PHARMACOLOGIQUE DES N-(ω-ALCOYLMERCAPTOALCOYL) -ADAMANTANE-1 CARBOXAMIDES ET LEURS AMINES CORRESPONDANTES.

DÉMETRIOS LAMBROU et POLYXENI TSITSA
Laboratoire de Pharmacie Chimique, 104, rue Solonos Athènes, 144-Grèce.
(Reçu le 4 Février 1978)

Resumé

Un certain nombre de nouveaux derivés de l'adamantane a été préparé et testé. Comparés à l'amantadine, ces produits ne présentent pas d'intérét à de rares exceptions près.

Key words: Dérivés de l'adamantane avec la S-alcoyl cystéamine et homocystéamine. Etude pharmacologique et comparaison avec l'amantadine.

Introduction

Les dernières années l'attention des chercheurs est tournée vers la structure de l'adamantane, qui introduit dans diverses molécules, a fourni des produits d'un intérêt majeur par rapport à ceux qui contenaient à sa place de restes d'hydrocarbures[1].

Par ailleurs, des auteurs ont décrit l'action de l'amino-1 adamantane (amantadine)[2] et plus récemment l'action antibiotique[3] de certains dérivés de formule générale suivante (I):

$$-CXNH\ (CHR)_n\ CXR' \qquad (I)$$

ou n=1, 5, 10 R=CH_3 ou H, R'=OH, X=S,O

A la suite de ces travaux et en considération avec notre mémoire[4] qui doit paraître aux Annales Pharmaceutiques Françaises, concernant de dérivés de la S-alcoylcystéamine et homocystéamine, nous avons estimé intéressant de procéder à la synthèse de deux séries suivantes II et III dont nous avons évalué le comportement pharmacologique:

$$CONH(CH_2)_nSR \qquad (II)$$

$$HCl$$

$$CH_2NH(CH_2)_nSR \qquad (III)$$

ou n=2,3 R=CH_3, C_2H_5, i-C_3H_7, n-C_4H_9

Les N-(ω-alcoylmercaptoalcoyl) adamantane-1 carboxamides, de formule

générale (II) ont été obtenus par action de la S-alcoylcystéamine et S-alcoylhomocystéamine 2 (n=2,3) sur le chlorure de l'acide adamantane-1 carboxylique. Les amines correspondantes (II), soit les (N-(ω-alcoylmercaptoalcoyl) méthyladamantane, ont été préparées à partir des amides II par reduction à l'acide d'hydrure de lithium-aluminium dans le THF. Les bases obtenues sont des huiles qui donnent des chlorhydrates bien cristallisés.

(Schéma 1)  COCl $H_2N(CH_2)nSR$ ⟶ (II) $\xrightarrow{LiAlH_4}$ (III)

1 *2*

Les amines 2, utilisées pour la synthèse ci-dessus ont été obtenues par deux méthodes différentes; c'est ainsi que les alcoylmercaptoéthyl-amines (2, n=2) ont été préparées par action des alcoylmercaptans correspondants sur l'ethylène-imine dans le méthanol,[4-6] tandis que les S-alcoyl-homocystéamines (2, n=3) ont été obtenues par action d'acrylonitrile sur le mercaptan correspondant en présence de méthylate de Sodium suivie d'une réduction à l'aide d'hydrure de lithium-aluminium.[4,7-9]

Le chlorure de l'acide adamantane-1carboxylique 1 a été préparé à partir de l'adamantane,[10] qui, traité par le brome conduit au bromo-1 adamantane[11]; l'action de l'acide formique dans l'acide sulfurique concentré[12] fournit l'acide qui est à son tour transformé en son chlorure[12] par action de chlorure de thionyle 1.

Au cours de l'action de ce dernier sur l'acide 1 en vu d'obtenir le chlorure, par chauffage et sans solvant, nous avons remarqué que le produit obtenu contenait du chlore mais ne montrait pas d'absorption de -CO à l'IR tandis que le point de fusion était différent de celui indiqué dans la littérature pour le chlorure. L'analyse et la comparaison avec un échantillon authentique de chloro-1adamantane (F: 168-170°) a montré qu'il agissait d'une décarbonylation. Ce cas est signalé dans la littérature[13] qu'il a lieu quand le produit est impur et cette degradation est attribuée à l'action catalytique de l'acide sulfurique qui se trouve comme impureté.

Bien que dans notre cas nous avons utilisé de l'acide adamantane-1 carboxylique très pur, nous n'avons pas obtenu le chlorure attendu dans les conditions expérimentales décrites plus haut. Nous avons pensé que cette anomalie était probablement due à la présence de l'acide chlorhydrique dans le chlorure de thionyle.

Afin de vérifier cette hypothèse nous avons effectué la réaction en utilisant du chlorure de thionyle purifié et dans un cas en y ajoutant une goutte d'acide chlorhydrique concentré.

Dans ce dernier cas nous avons obtenu le chloro-1adamantane (F:168-170°), vérifié par l'analyse et le spectre I.R., tandis que dans les autres cas, le chlorure de l'acide adamantane-1 carboxylique était normalement obtenu.

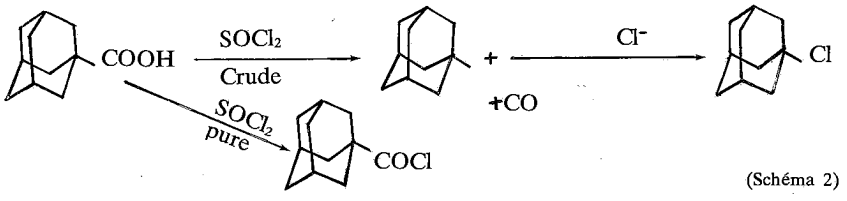

(Schéma 2)

Cette observation nous amène à penser que la prèsence d'un acide fort catalyse la formation de l'ion carbonium[15] et conduit à l'observation du dérivé chloré, (Schéma 2).

Partie Expérimentale

Les points de fusion ont été pris dans un appareil de Büchi, et ne sont pas corrigés. Les analyses ont été effectuées au Service Central de Microanalyse du S.N.R.S. et au Laboratoires Ciba que nous remercions vivement. Les résultats des microanalyses se trouvent dans les limites ± 0,4% des valeurs calculées. Les spectres IR ont été enregistrés à l'aide d'un appareil de Beckman IR-4.

I. S-alcoyl-cystéamines et homocystéamines 2.

a) Alcoylmercaptoéthylamines[4-6] *2* (n=2). Elles ont été préparées par action du mercaptan approprié sur l'éthylène imine dans le méthanol à -15°. On laisse au repos une nuit à t° ambiante.

b) Alcoylmércaptopropylamines[4,7-9] *2* (n=3). Elles ont été obtenues par action d'acrylonitrile sur le mercaptan approprié en présence de méthylate de sodium dans le benzène anhydre à 0°, suivi d'une reduction des nitriles obtenus par l'hydrure de lithium-aluminium dans l'éther anhydre.

II. Chlorocarbonyl-1 adamantane 1.

a) Bromoadamantane[11]. Un mélange de 25g d'adamantane[10] et de 35ml de brome est agité énergiquement et chauffé progressivement dans un bain d'huile jusqu'à 110°. On maintient cette t° pendant 5h après quoi le mélange est repris par 100ml de tetrachlorure de carbone et versé dans glace-eau. Le récipient est bien lavé par 50ml du même solvant qui est versé dans le mélange. On fait passer un courant de gaz sulfureux jusqu'à décoloration, on sépare les deux couches, extrait la couche aqueuse au tetrachlorure de carbone et les solutions reunies sont séchées et le solvant évaporé sous vide en chauffant à 50°. Le résidu solide est dissous à chaud dans 40ml de méthanol qui par refroidissement laisse 37g de produit cristallisé qui fond à 115-117°.

b) Acide adamantane-1 carboxylique[12]. Il a été préparé par la méthode de Stetter *et coll*[12]. Avec quelques modifications 12g de 1-bromoadamantane bien pulverisés sont mis en suspension dans 300ml d'acide sulfurique concentré refroidi à 10° dans la glace. On retire le bain froid et on fait couler goutte à goutte sous forte agitation mécanique 50ml d'acide formique anhydre. Le bromoadamantane se dissous au fur et à mésure. La réaction dure 4 heures. On filtre à travers du coton de verre et verse le liquide dans la glace. Le solide séparé est purifié par dissolution dans une solution d'hydroxyde de sodium à 5% et reprécipité par acidification. Rendement 96%, F:181°.

c) Chlorure de l'acide adamantane-1 carboxylique[12]. On chauffe pendant 1 heure à 50-60° un mélange de 18g d'acide adamantane-1 carboxylique pur et 20g de chlorure de thionyle, puis élimine l'excès du réactif, ajoute du benzène et évapore de nouveau le solvant pour enlever les traces du $SOCl_2$. Le résidu est un solide blanc qui fond à 54-56° (litt. 54-56°). Rendement 99%.

N-(ω-Alcoylmercaptoalcoyl) adamantane-1 carboxamides (II). Une solution (0,01 mole) de chlorure 1 dans 50 ml d'éther anhydre est ajouté goutte à goutte et sous agitation mécanique dans une solution (0,02 mole) de l'amine dans 100 ml d'éther anhydre, refroidie dans l'eau. Après addition du réactif on poursuit l'agitation pendant 15 min. On sépare la couche organique, lave à l'eau, sèche sur $MgSO_4$ et évapore le solvant. On obtient ainsi un produit solide que l'on recristallise dans un solvant approprié (voir le tableau I).

TABLEAU I

No	R	n	Rtd%	F°C[a]	FORMULE MOLECULAIRE	IR ABSORPTION[b] cm^{-1}>C=0	Analyse C% Calc.	C% Tr.	H% Calc.	H% Tr.	N% Calc.	N% Tr.	S% Calc.	S% Tr.
1	CH_3	2	92	92-94	$C_{14}H_{23}NOS$	1625	66,36	66,46	9,15	9,14	5,53	5,55	12,65	12,68
2	CH_3	3	93	107-109	$C_{15}H_{25}NOS$	1620	67,38	67,27	9,42	9,48	5,24	5,21	11,99	11,90
3	C_2H_5	2	88	73-75	$C_{15}H_{25}NOS$	1625	67,38	67,31	9,42	9,53	5,24	5,22	11,99	11,97
4	C_2H_5	3	89	68-70	$C_{16}H_{27}NOS$	1620	68,26	68,16	9,67	9,65	4,98	4,99	11,39	11,41
5	$C_3H_{7\text{-}i}$	2	82	84-86	$C_{16}H_{27}NOS$	1625	68,26	68,19	9,67	9,57	4,98	4,92	11,39	11,45
6	$C_3H_{7\text{-}i}$	3	90	46-48	$C_{17}H_{29}NOS$	1620	69,10	69,21	9,91	9,92	4,74	4,68	10,85	10,88
7	$C_4H_{9\text{-}n}$	2	89	48-50	$C_{17}H_{29}NOS$	1625	69,10	69,24	9,91	9,89	4,74	4,80	10,85	10,83
8	$C_4H_{9\text{-}n}$	3	93	63-65	$C_{18}H_{31}NOS$	1620	69,85	69,82	10,09	10,19	4,53	4,60	10,36	10,41

[a]Recristallisation dans un mélange benzène - éther de pétrole.
[b]Les spectres IR ont été obtenus dans les Nujol.

TABLEAU II

No	R	n	Rtd%[a]	F°C[b]	FORMULE MOLECULAIRE	Analyse C% Calc.	C% Tr.	H% Calc.	H% Tr.	N% Calc.	N% Tr.	S% Calc.	S% Tr.	Cl% Calc.	Cl% Tr.
1	CH_3	2	90	268-270 dec	$C_{14}H_{25}NS.HCl$	60,94	60,90	9,50	9,52	5,09	5,10	11,62	11,55	12,85	12,88
2	CH_3	3	83	226-228	$C_{15}H_{27}NS.HCl$	62,14	62,22	9,73	9,69	4,84	4,76	11,06	11,10	12,23	12,35
3	C_2H_5	2	78	252-254 dec	$C_{15}H_{27}NS.HCl$	62,14	62,09	9,73	9,68	4,84	4,89	11,06	11,07	12,23	12,29
4	C_2H_5	3	86	184-186	$C_{16}H_{29}NS.HCl$	63,23	63,25	9,95	9,96	4,61	4,71	10,55	10,45	11,66	11,68
5	$C_3H_{7\text{-}i}$	2	89	256-258	$C_{16}H_{29}NS.HCl$	63,23	63,28	9,95	9,97	4,61	4,59	10,55	10,61	11,66	11,70
6	$C_3H_{7\text{-}i}$	3	85	212-214 dec	$C_{17}H_{31}NS.HCl$	64,22	64,30	10,14	10,24	4,41	4,39	10,08	10,12	11,15	11,25
7	$C_4H_{9\text{-}n}$	2	84	232-234	$C_{17}H_{31}NS.HCl$	64,22	64,32	10,14	10,20	4,41	4,51	10,08	10,20	11,15	11,30
8	$C_4H_{9\text{-}n}$	3	89	184-186	$C_{18}H_{33}NS.HCl$	65,13	65,12	10,32	10,36	4,22	4,20	9,65	9,75	10,68	10,76

[a] Les rendements sont calculés en chlorhydrate pur. [b]Après recristallisation dans un mélange d'éthanol absolu-éther anhydre.

N-(ω-Alcoylmercaptoalcoyl)-aminométhyladamantane-1 (III). Une solution (0,012 mole) de l'amine II dans 60 ml de tetrahydrofurane anhydre est ajoutée goutte à goutte dans une suspension agitée d'hydrure de lithium-aluminium (0,013 mole) dans 60 ml de tetrahydrofurane. Le mélange est chauffé à reflux pendant 2-3 heures. Après refroidissement il est décomposé avec de l'eau alcaline (0,5 ml d'eau + 0,5 ml de NaOH 15%). On filtre le minéral, lave bien au THF et le solvant est évaporé sous vide par léger chauffage. Le résidu est une huile qui est transformée en chlorhydrate.

Les analyses et les constantes se trouvent dans le tableau II.

Etude Pharmacologique

Ces produits des formules générales II et III (voir Tableau I et.II) ont été soumis à un screening pharmacologique destiné à révéler leur toxicité et leurs éventuelles activités sédative[16-17], psychotrope[18-19] et analgésique[20].

Leur toxicité aigüe est faible: supérieure ou égale à 550 mg/kg chez la souris per os.

Les produits étudiés ne possèdent pas les propriétés remarquables de l'amantadine.

En effet, à de rares exceptions près, leur activité s'est révélé inférieure.

Toutefois, l'essai des produits No 1 (Table II) et No 7 (Table I) a montré une augmentation de l'activité chez le rat qui est égale ou même supérieure à celle de l'amantadine.

Il en est de même pour les produits No 2 et No 3 (Table II) quant à la potentialisation de la toxicité du penétrazol.

Enfin les produits No 1 et No 2 (Table II) s' avèrent actifs sur la diminution de la catalepsie chez le rat à des doses comparables à celle de l'amantadine.

Remerciements

Nous remercions très vivement Mr. R. Cholet, Pharmacologue du Centre de Recherches Sauba (France) qui a bien voulu faire pour nous l'étude pharmacologique.

Abstract

N-(ω-alkyl mercaptoalkyl) -adamantan-1 - carboxamides and amines (II and III).

Reaction of S-alkyl cysteamine or homocysteamine with equimolar of adamantane carbonyl chloride in the presence of sodium carbonate in ether gave the corresponding amides in good yield. Reduction of the amides (II) with $LiAlH_4$ in THF gave the amines (III) as oils, which were converted to their crystalline hydrochloric salts.

A comparison of their pharmacological activity to that of amantadine is discussed.

Περίληψις

N-(ω-ἀλκυλο-μερκαπτοαλκυλο) -ἀδαμαντανο-1-καρβοξαμίδια καὶ ἀμῖναι (II καὶ III).

Εἰς τὴν ἐργασίαν αὐτὴν περιγράφεται ἡ σύνθεσις N-(ω-ἀλκυλο-μερκαπτοαλκυλο) -ἀδαμαντανο-1-καρβοξαμιδίων (II) καὶ τῶν ἀντιστοίχων ἀμινῶν (III). Τὰ προϊόντα (II) ἐλήφθησαν μὲ καλὴν ἀπόδοσιν, δι' ἀντιδράσεως ἰσομοριακῶν ποσοτήτων S-ἀλκυλο κυστεαμίνης καὶ ὁμοκυστεαμίνης ἐπὶ τοῦ χλωριδίου τοῦ ἀδαμαντανικοῦ ὀξέος, ἐντὸς αἰθέρος, παρουσία ἀλκαλικοῦ μέσου (Na_2CO_3). Ἐκ τῶν οὕτω ληφθέντων προϊόντων (II), δι' ἀναγωγῆς μετὰ $LiAlH_4$ ἐντὸς THF, ἐλήφθησαν αἱ ἀντίστοιχοι ἀμῖναι (III) αἱ ὁποῖαι ἦσαν ἐλαιώδεις καὶ μετετράπησαν εἰς τὰ ἀντίστοιχα ὑδροχλωρικὰ ἅλατα αὐτῶν, τὰ ὁποῖα ἦσαν στερεὰ κρυσταλλικὰ σώματα. Ἀνακοινοῦνται ἐπίσης τὰ ἀποτελέσματα τῆς φαρμακολογικῆς ἐκτιμήσεως ἐν συγκρίσει πρὸς τὴν ἀμανταντίνην.

Bibliographie

1. Gerzon K., Tobias D.J., Holmes R.E., Rathbun R.E., et Kattu R.W.: *J. Med. Chem.*, **10**, 603 (1967).
2. Runti C.R.: *Farmaco, Ed. Sci.*, **22**, 953 (1967).
3. Krimmel C.P.: pat. U.S. 3,624,086 (1971); *Chem. Abstr.*, **76**, 59651 K (1972).
4. Lambrou D., et Tsatsas G.: *Ann. Pharm. Fr.*, **32**, 295-300 (1974).
5. Tsatsas G., Sandris C., et Kontonasios D.: *Bull. Soc. Chim. Fr.*, p. 3100 (1964).
6. Wieland T., Moeller E.F., et Dieckelmann, G.: *Ber.*, **85** 1035 (1952).
7. Hurde C.D., et Gerschbein L.L.: *J. Am. Chem. Soc.*, **69**, 2328 (1947).
8. Kjaer A., Marcus F., et Conti J.: *Acta Chem. Scand.*, **7**, 1370 (1953).
9. Tsatsas G., Sandris C., et Contonasios D.: *Bull. Soc. Chim. Fr.*, p. 2160 (1963).
10. Schleyer P.R.: *J. Am. Chem. Soc.*, **79**, 3292 (1957).
11. Stetter H., Schwarz M., et Hirschorn A.: *Ber.*, **92**, 1629 (1959).
12. Stetter H., Rauscher E.: *Ber.*, **93**, 1161 (1960).
13. Fieser L.F., Nazer M.Z., Archer S., Berberian D.A., et Slighter R.G.: J. *Med. Chem.*, **5**, 517 (1967).
14. Fieser L.F., et Fieser M., *"Reagents for Organic Synthesis" p. 1158* John Wiley and Sons, Inc., New York, N.Y., (1967).
15. Forte R.C., et Schleyer P.V.: *Chem. Rev.*, **64**, 277 (1964).
16. Dews P.B.: *Brit: J. Pharmacol.*, **8**, 46 (1953).
17. Boissier J.R., Simon P.: *Arch.Int.Pharmacodyn.*, **158No1**, 212-221 (1965).
18. Rubin B., Malone M.H., Vauglis M.H., Burke J.C.: *J. Pharmacol.*, **120**, 125-136 (1957).
19. Boissier J.R., Simon P.: *Thérapie*, **18**, 1257-1277 (1963).
20. Siegmund E., Cadmus R., Lu G.: *Proc.Soc. Exper.Biol. and Med.*, **95**, 729 (1957).

Chimika Chronika, New Series. 7, 203-213 (1978)

TRANSIENT SPECIES IN THE PHOTOLYSIS OF 2-NITRO-BENZYLIDENE-HYDRAZIDES AND RELATED COMPOUNDS

E. HADJOUDIS, I. ARGYROGLOU and A. TSOKA
Chemistry Department Nuclear Research Center "Demokritos", Athens, Greece
(Received February 17, 1978)

Summary

The spectra and photochemistry of 2-nitro-benzylidene-isonicotinic hydrazide and some related compounds have been investigated in the crystalline state, in rigid glasses and in solution.

Coloured transient species have been detected by flash photolysis experiments. The photochromic process seems to involve an intramolecular hydrogen abstraction by the nitro group in the case of 2-nitrobenzylidene-isonicotinic hydrazide and a tautomeric benzenoid quinonoid equilibrium in the case of 2-hydroxybenzylidene-pyridine-4-carboxylic acid hydrazide.

Kew words: Photochemistry, flash photolysis, photochromism, keto-enol phototautomerism, hydrogen abstraction.

Introduction

Many aromatic nitro compounds which change their colour on irradiation are described in the literature.[1] Most of them are substituted in the *ortho* position to the nitro group and in 1904 Sachs and Hilpert[2] formulated the following rule (known as the Sachs rule).

"All aromatic nitro compounds, which contain in a position *ortho* to the nitro group a CH group are lightsensitive".

However, although the proximity of the nitro group and the side chain seems to be a condition for lightsensitivity, there are other factors which also govern the photochemical behaviour and mechanism of such reactions; for instance the photochemical isomerisation (I) observed[3] in the crystalline state 25 years ago is still a matter of controversy. Thus Ellan *el all*[4] studied again the photochromic properties of a number of 2-nitrobenzylidene - pyridine carboxylic acid hydrazides (II) with R = H, 4-NO_2, 5-OH and 5-OMe. Of this series, 2-nitrobenzylidene-pyridine-4-carboxylic acid hydrazide (R = H) showed on irradiation with UV-light a rapid colour change from pale-yellow to red. The colour change reverses thermally in the dark. The above workers were able to follow the reaction in the

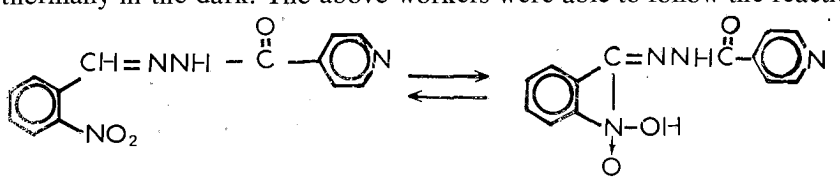

(I)

crystalline state only and suggested a mechanism which involves a shift via an excited state in the double bond sequence (III).

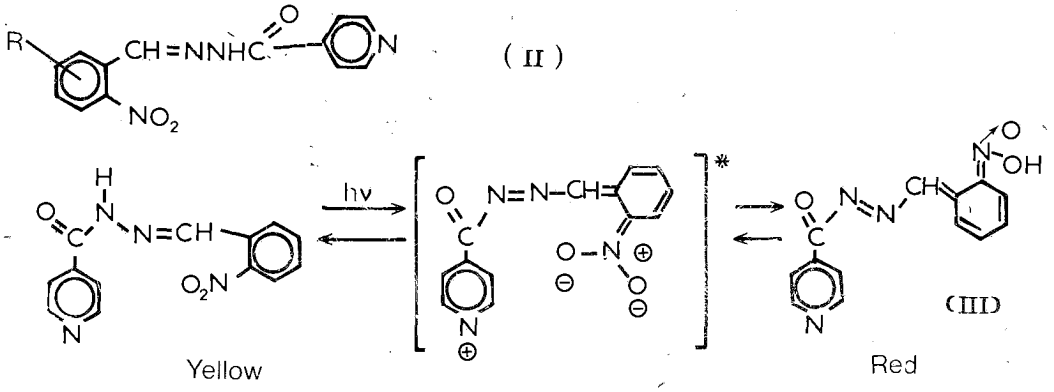

In a more recent publication[5] evidence is presented, based on the mass spectra of substituted aroylhydrazones that structure (IV) is also possible for the photoproduct (although this was excluded from previous workers[3]).

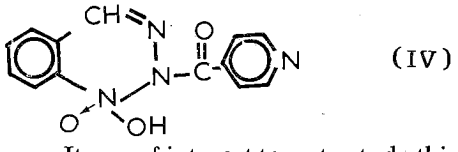

It was of interest to us to study this and other relative compounds since (i) we have studied[6] the solid-state photochemical rearrangement of the relative compound of *ortho*-nitrobenzylideneaniline (V) and (ii) we observed[7] photochromic phenomena in the related compounds of benzenesulfonyl hydrazones of salicylaldehyde (VI).

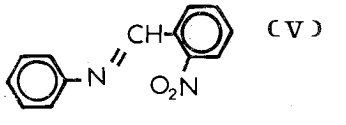

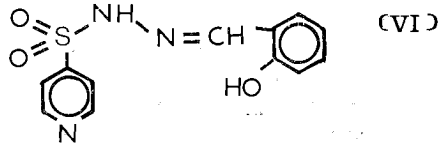

Finally it was desirable (to us) to study by the flash photolysis technique the photochromism of (I) in solution which was not observed before and evaluate the mechanism(s) involved.

Experimental

The compounds 2-nitrobenzylidene-pyridine-4-carboxylic acid hydrazide (1), benzylidene-pyridine-4-carboxylic acid hydrazide (2) and 2-hydroxybenzylidene-pyridine-4-carboxylic acid hydrazide (3) were prepared by condensation of isonicotinic acid hydrazide and the corresponding benzaldehyde in ethanol. 2-Nitrobenzaldehyde benzoyl hydrazone (4), 2-hydroxybenzaldehyde benzoyl hydrazone (5) and benzaldehyde benzoyl hydrazone (6) were prepared by condensation of aroylhydrazine and the corresponding benzaldehyde in ethanol. All the compounds were purified by repeated recrystallizations from ethanol and reflected good elemental analysis.

The rigid-state experiments were conducted with solutions in EPA (ether: isopentane: alcohol, 1:5:5) at liquid nitrogen temperature and in polymerised methyl methacrylate (PMMA) at room temperature and at liquid nitrogen temperature. No correction was made to the spectra for contraction of the solution on cooling as this was found to be less than 10% in EPA and of the order of 5% in PMMA.

PMMA solutions were prepared by dissolving the compounds in distilled methyl methacrylate which was then polymerised in air at about 80°C. The polymer samples were cut and polished to give cylinders of approximately 10mm diam and 5-10mm length. Initiator $a_1\acute{\alpha}$ azodiisobutyronitrile, 0.00 1% (w/w) was added. Solute in methyl methacrylate prior to polymerisation.

Absorption spectra were recorded on a Cary Model 17 spectrophotometer.

A quartz Dewar vessel with quartz windows was used for the measurement of optical spectra in rigid glasses at low temperature.

Crystalline films were prepared from the melt between two quartz plates under pressure.

Steady state irradiations were carried out (i) with an immersion medium pressure Hg UV lamp, and (ii) with a 200W high-pressure Hg UV lamp and appropriate filters.

Compounds 1 and 4 were irradiated in the crystalline state with a full mercury arc. The flash photolysis apparatus (Hivotronic, England), permits the direct observation of the triplet state decay as a function of time for various molecules. An extremely intense flash produced by two vertical quartz photolysis lamps (200mm long of 10mm diameter filled with 6 cm pressure of krypton) triggered by an 8 microfarad capacitor charged to 12 kilovolts, falls on the sample solution in a 20 cm optical cell placed between the two photolysis lamps. The photolytic flash has a half-height width of about 30μsec. A quartz-idine lamp, above the sample cell, is used as a constant intensity monitoring source which induces $T_1 \rightarrow T_n$ transitions in the excited molecule. Recording the transmitted lamp intensity as a function of time (at a certain wavelength) gives a decay curve since more light is transmitted by the sample as the concentration of excited species decreases. From this decay curve, the decay time and the rate constant (K_1 or K_2) is evaluated with an appropriate computer program. The above mentioned wavelenght is set by a Hilger Watts monochromator capable of providing monochromatic light anywhere between 0 and 999 nm; the recording of the transient is attained with the help of an oscilloscope (Tektronix model 545 B) equipped with a polaroid camera.

Results

Crystalline state.

By screening the compounds (in the form of polycrystalline powders) for photochromic and thermochromic properties we found the results shown in Table I.

Rigid Glasses.

Compounds 1, 2, 4 and 6 present no photochromic (or thermochromic) behaviour on irradiation with UV-light in EPA or in PMMA at liquid nitrogen temperature. However, compound 1, on irradiation at room temperature in PMMA shows a drop in its absorption spectrum irreversibly.

Compounds 3 and 5 produce no change on irradiation in EPA. On cooling

TABLE I. *Photochromic and Thermochromic Properties of Polycrystalline Benzylidene-acyhydrazides.*

No.	Compound	Effect of Light	Effect of Heat	Fluo-re-sence	colour change
1	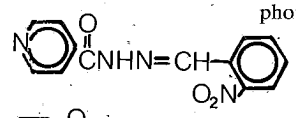	photochromic[a]	—	no	pale yellow → Red[c]
2	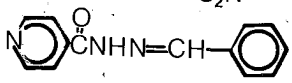	—	—	no	
3	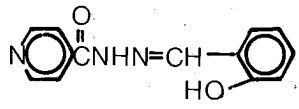	—	themochromic[b]	yes	whitish → Yellow[c]
4	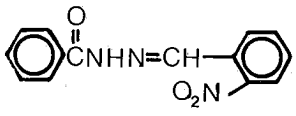	photochromic[a]	—	no	pale yellow → Red[c]
5	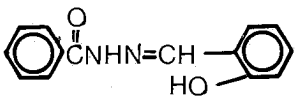	—	thermochromic[b]	yes	whitish → Yellow[c]
6	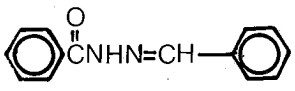	—	—	no	

a. the colour change reverses experimentally slowly in the dark. The reversal time is faster at higher temperatures.
b. the compounds are heated below their m.p. and cooled down to liquid nitrogen temperature.
c. all the coloured forms are non-fluorescent.

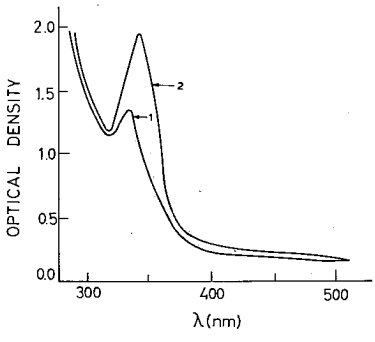

FIG. 1: *Spectra of a 10^{-4}M solution of compound 3 in EPA.* 1, at room temperature; 2, at liquid nitrogen temperature; after softening of the rigid solution, the spectrum returns to 1.

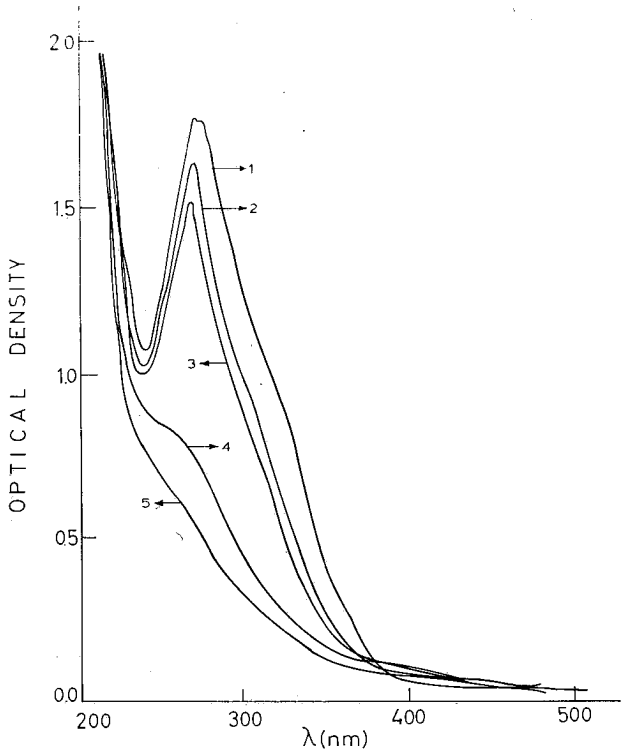

FIG. 2: *Spectra of a 10^{-4}M solution of compound 1 in methanol.* 1, before irradiation; 2, after 3 min of irradiation; 3, after 6 min of irradiation; 4, after 30 min of irradiation; 5, after 90 min of irradiation. (All irradiations with immersed lamp).

however, down to liquid nitrogen temperature, the existing band at 335nm is shifted to 345nm and becomes much stronger. On softening (RT) the spectrum returns to the original. These results are shown in Fig. 2.

Solution Photochemistry.

Steady state irradiation of ethanolic or methanolic solutions of compound 1 at room temperature causes irreversible changes in the absorption spectra. Fig. 2 shows the results at various steps of the irradiation. Although the photoproducts were not identified T.L.C. showed, except from the parent compound 1, two additional components. Compound 4 behaves in a similar way. Compounds 3 and 5 do not decompose on irradiation but undergo minor changes. Thus, a very weak band appears at about 400nm with a simultaneous small drop of the spectrum in the lower region. This behaviour is reversible, thus the spectrum returns slowly to the original in the dark. This is shown in Fig. 3 for the case of compound 3. It should be noted that the weak band at about 400nm is also formed in polar aprotic solvents without irradiation and in lower concentrations. These are shown in Figs. 4 and 5 again for compound 3. These features are not present in the compounds 4, 2 and6.

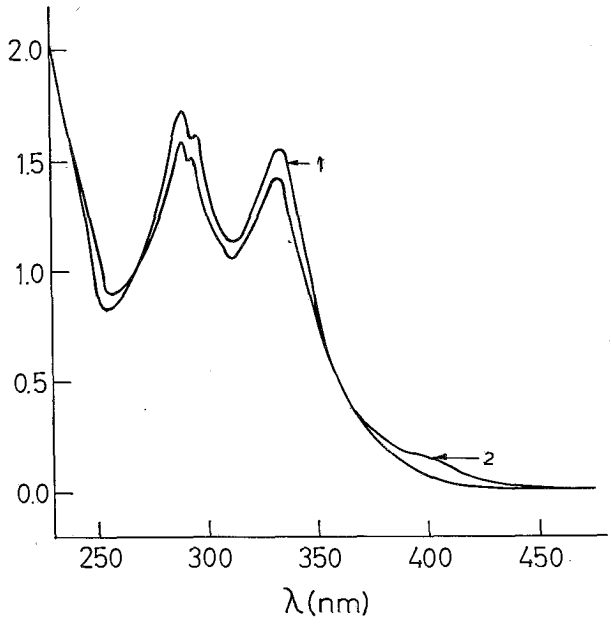

FIG. 3: *Spectra of a 10^{-4}M solution of compound 3 in ethanol.* 1, before irradiation; 2, after 10 min of irradiation. Irradiation for longer period of time brings no more change in the spectrum. Spectrum 2 returns to 1 on standing in the dark.

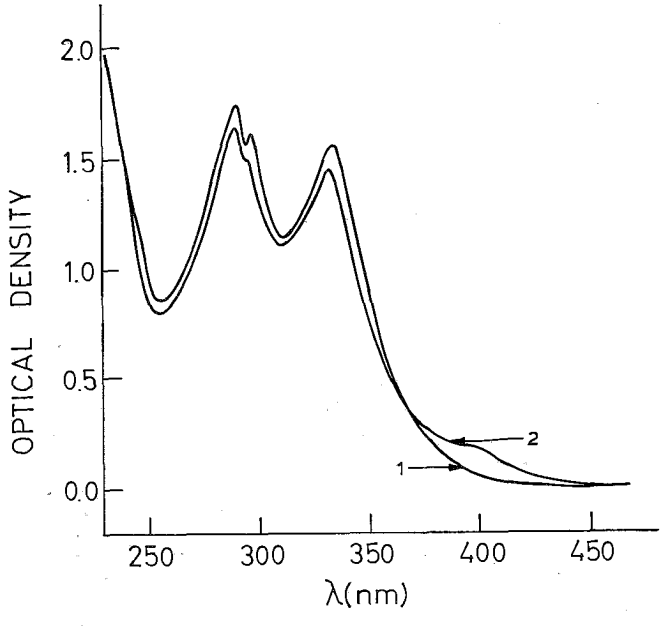

FIG. 4: *Spectra of 5.10^{-4}M solution of compounds 3.* 1, in ehtanol; 2, in DMF.

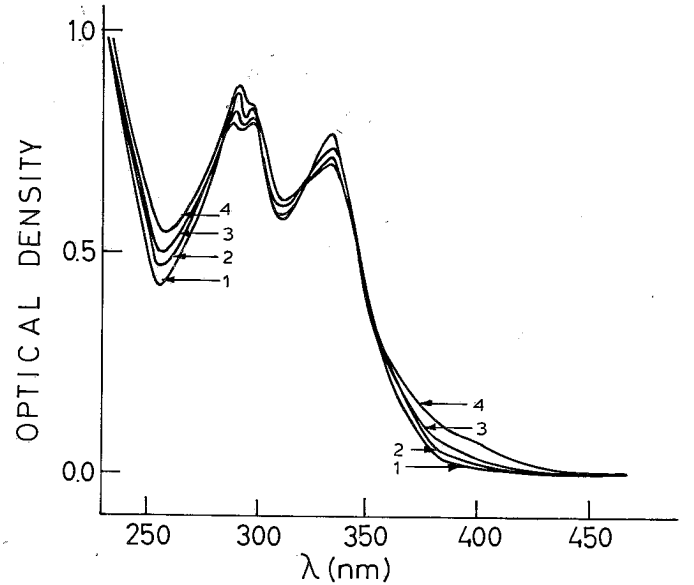

FIG. 5: *Spectra of compound 3 at various concentrations in ethanol.* 1, $5 \cdot 10^{-4}$M in a 0.1cm-cell; 2, $2.5 \cdot 10^{-4}$M in a 0.2cm-cell; 3, 5.10^{-4}M in a 1cm-cell; 4, 10^{-5}M in a 5cm-cell.

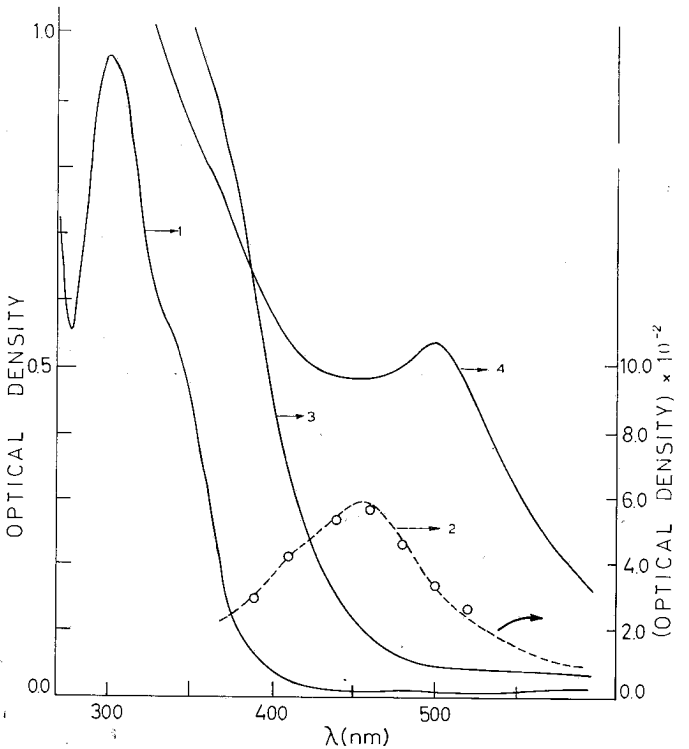

FIG. 6: *Spectra of a 10^{-4}M solution of compound 1 in PMMA at room temperature.* 1, in PMMA; 2, transient spectrum in PMMA; 3, thin polycrystalline film; 4, irradiated thin polycrystalline film for 1h.

Flash Photolysis.
Compound 1 in a 10^{-4}M solution in PMMA (at room temperature) develops a transient with a half-life of about 150m sec and which has its maximum absorption at about 455nm. The transient decays with first-order kinetics. From the plots of loglog (I_∞/I) vs. time at different wavelengths, the absorption spectrum of the transient could be calculated and it is given in Fig. 6 together with the spectra of compound 1 in PMMA and in a thin polycrystalline film for reasons of comparison.

The transient spectrum obtained by flash photolysis of compound 1 in 10^{-4}M ethanol shows a maximum near 400nm comparable to the spectra for compound 1 irradiation at room temperature PMMA glass shown in Fig. 7. This transient has a half-life of about 50msec. It should be noted, however, that this transient is secondary since it appears after the first flash and becomes stronger as the number of flashes increases. On subsequent flashing the intensity of the transient starts to drop until no more transient is observable. The behaviour is similar with steady-state irradiation, thus a pre-irradiated solution (e.g. irradiated for 5 min. with the immersion Hg lamp) developes the transient while vanishes in a solution which has been irradiated for 30 min. with the immersion lamp.

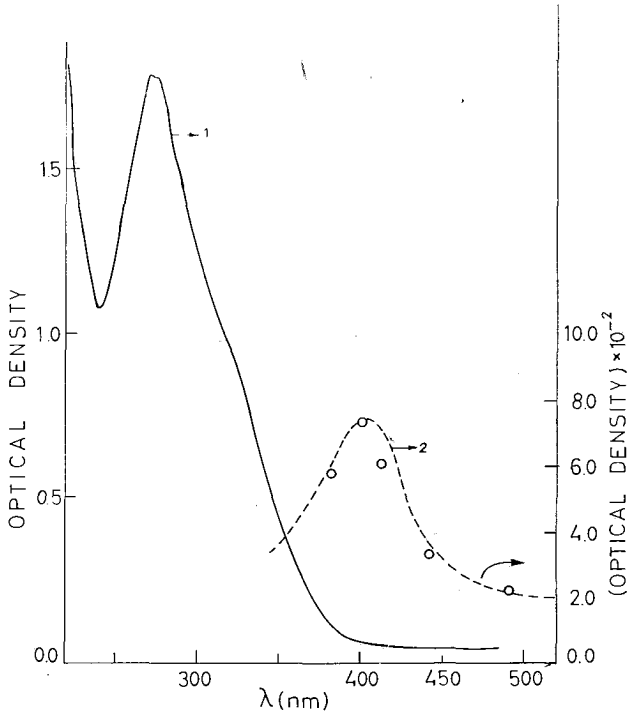

FIG. 7: *Spectra of a 10^{-4}M solution of compound 1 in ethanol.* 1, in ethanol; 2, transient spectrum.

Compound 4 behaves in a similar way.

Compound 3, on flashing, developes a transient which decays with first-order kinetics with $K_1 = 1.8 \cdot 10^{-3}$ sec^{-1} and has an absorption spectrum with maximum at about 400nm. Compound 5 behaves similarly.

Compounds 2 and 6 do not show any transient under our flashing conditions but some product formation is observed in agreement with that formed under steady-state irradiation. Table 2 shows the first-order rate constants (K_1) and the decay half-time ($t\frac{1}{2}$) at 400nm in 10^{-4} solutions in ethanol for the compouns studied.

TABLE II: *First-order Rate Constants (K_1) and Decay half-time ($t\frac{1}{2}$) at 400 nm in 10^{-4}M Solutions in Ethanol*

Compound	K_1 (10^{-3} sec^{-1})	$t\frac{1}{2}$ (msec)
1	13.8	50
2	—	—
3	1.8	380
4	11.5	60
5	1.7	400
6	—	—

Discussion

The transient absorption spectra of compounds 3 and 5 suggest that these compouns behave in solution like their analoghes of benzenesulfonyl hydrazones of salicylaldehyde[7] and therefore the coloured transients are attributed to the quinoid species of the tautomeric benzenoid quinonoid species of the tautomeric benzenoid quinonoid equilibrium (VII).

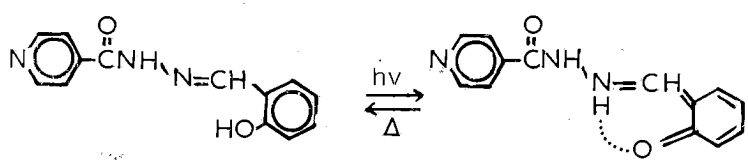

(VII)

We turn now to compound 1 which was the main target of the present investigation.

As it was noted by previous workers[4], the reversible photochromic reaction in the crystalline state, was not observed in solution using conventional methods. However, with the flash photolysis technique in the present work we observed coloured transients which, in the case of PMMA rigid solution was attributed to the same colured species as in the crystalline spectrum (compare the transient absorption spectrum in Fig. 6 with that of the polycrystalline film). The transient spectrum is blue shifted (by about 40nm) and although no theoretical interpretation seems to be available of such shift, it might result from the combined effects of a small real shift and of substantial broadening of the longest absorption bands; both effects are reflected in the values of wavelenght at which the absorbance has half its peak value ($\Delta\lambda 1/2$) at the long wavelenght edge[8]. The photochemical reaction responsible for the formation of the coloured transient species appears to involve (in the case of compounds 1 and 4) a hydrogen abstraction by the nitro group.

Because of the proximity of the CH group, the abstraction proceeds intramolecularly with a first-order rate constant leading to a change in the structure of the aromatic ring to a quinoid configuration as shown in (VIII) for the case of compound 1.

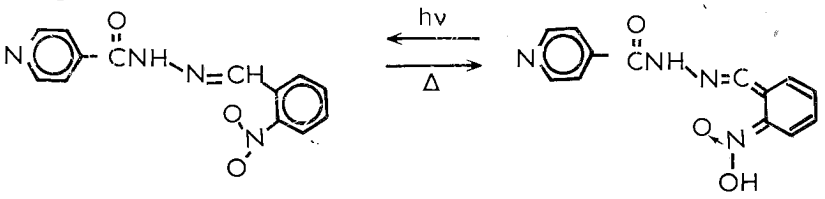

(VIII)

The above mechanism is supported by a number of studies with nitro-compounds which have yielded transient spectra indicative of aci-nitro derivatives[9]. The presence of these species can be explained by hydrogen abstraction by the excited nitro group to yield the unstable derivative as in the examples shown in (IX), (X) and (XI)[10, 11, 6]

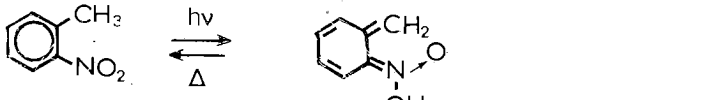

(IX)

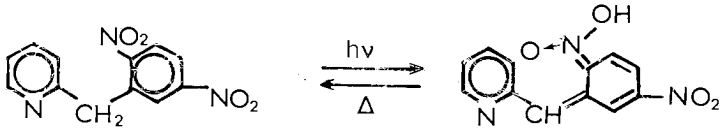

(X)

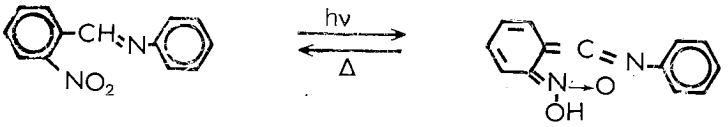

(XI)

However the possibility of hydrogen abstraction from the NH group as it was previously suggested[4] should not be excluded and as it was mentioned in the introduction, the possiblity of both =CH- and NH groups acting as reactive centers has been demonstrated[5].

A comment is deserved for the temperature effect of compound 3 shown in Fig. 1 and for the appearance of a small band at about 400nm (compounds 3 and 5) in the cases of Figs. 3, 4 and 5. The results of Fig. 1 may be explained from the fact that as lower temperatures are approached, the deviation from planarity tends to become less, possibly because of the lowering of thermal energy and increased cappacity of the molecule to remain in a strained configuration[12]. *The 400nm small band (Figs. 3, 4 and 5) is probably due to the n-π^* transition of the C = O group.* H-bonded C = O does not show this band, thus the concentration and the aprotic polar solvent effect.

Acknowledgment.

We wish to thank Mrs. S. Philippakopoulou for her valuable technical assistance.

Περίληψη

Ἐνδιάμεσα βραχύβια προϊόντα κατὰ τὴν φωτόλυση τοῦ 2-ὑδρο-ξυβενζυλιδενο-ἰσονικοτινικοῦ ὑδραζιδίου καὶ ἄλλων σχετικῶν ἑνώσεων.

Στὴν ἐργασία αὐτὴ μελετήθηκαν, κυρίως μὲ τὴν τεχνικὴ τῆς παλμικῆς φωτολύσεως, διάφορα βενζυλιδένο ὑδραζίδια καὶ ἄλλες σχετικὲς ἑνώσεις στὴν κρυσταλλικὴ κατάσταση, σὲ ὑαλώδη διαλύματα καὶ σὲ διαλύματα.

Στὰ διαλύματα παρατηρήθηκαν ἔγχρωμα βραχύβια προϊόντα, τὰ ὁποῖα δείχνουν τὴν ὕπαρξη φωτοχρωμισμοῦ. Ὁ φωτοχρωμισμὸς στὴν περίπτωση τοῦ 2-ὑδροξυβενζυλιδένο ἰσονικοτινικοῦ ὑδραζιδίου φαίνεται νὰ ὀφείλεται στὴ μεταφορὰ πρωτονίου καὶ στὸ σχηματισμὸ μορίων μὲ κινοειδῆ μορφὴ καὶ στὴν περίπτωση τοῦ 2-νιτροβενζυλιδένο ἰσονικοτινικοῦ ὑδραζιδίου στὴν ἀπόσπαση ὑδρογόνου τῆς νιτροομάδας ἀπὸ τὴν ὁμάδα -CH= τῆς ὀρθο-θέσεως.

References and Notes

1. Coppens, Ph., Ph. D. Thesis, Amsterdam University, 1960.
2. Sachs, F. and Hilpert, S.: *Ber.*, **37**, 3425 (1904).
3. Mattu, F., Parisi, R. and Manca, M.: *Ann. Chim., (Rome)*, **42**, 632 (1952); *Chem. Abstr.*, **47**, 12382b (1953); Mattu, F. and Mascia, C.: *Rend. Seminario Fac. Sci. Univ. Cagliari*, **34**, 207 (1964); *Chem. Abstr.*, **63**, 15756h (1956).
4. Ellan, R.M., East, P.B., Kelly, A., Khan, R.M., Lee, J.B. and Lindsey, D.C.: *Chem. and Ind.*, **74** (1974).
5. Alexandrou, N.E. and Stephanidou - Stephanatou, J.: *Chimika Chronika, (New Series)*, 6, 357 (1977).
6. Hadjoudis, E. and Hayon, E.: *J. Phys. Chem.*, **74**, 2224 (1970); *J. Phys. Chem.*, **74**, 3184 (1970).
7. Hadjoudis, E. and Gegiou - Hadjoudis, D.: *Chimika Chronika (New Series)* **4**, 51, (1975).
8. Goedicke, C., Stegemeyer, H., Fiscer, G. and Fischer, E.: *Zeitschrift für Physikalische Chemie (NF)* **101**, 181 (1976).
9. Wettermark, G.: *J. Am. Chem. Soc.*, **84**, 3658 (1962); Wettermark, G.: *J. Phys. Chem.*, **66**, 2560 (1962); Wettermark, G.: *Photochem. Photobiol.*, **4**, 229 (1965).
10. Cowan, D.O. and Drisko, R.L., *"Elements of Organic Photochemistry"*, p. 128 Plenum Press, New York and London, 1976.
11. Margerum, J.D., Miller, L.J., Saito, E., Brown, M.S., Mosher, H.S. and Hardwick, R.: *J. Phys. Chem.*, **66**, 2434 (1962).
12. Sheppard, S.E. and Brigham, H.R.: *J. Am. Chem. Soc.*, **66**, 380 (1944).

Chimika Chronika, New Series, 7, 215-219 (1978)

COMPARATIVE STUDY ON THE ADSORPTION DATA OF URIC ACID ON DIFFERENT TYPES OF CHARCOAL AND MANGANESE DIOXIDE

H. TSOUKALI-PAPADOPOULOU, A. PAPADIMITRAKI-NATHANAEL and B.K. NATHANAEL

Department of Legal Medicine and Toxicology, Medical Faculty, Aristotelian University of Thessaloniki, Dir.: Prof. A. Theodossiou and Laboratory of Clinical Chemistry, AXEPA Hospital, Thessaloniki, Dir.: Prof. A. Trakatelis.

Summary

(Received February 17, 1978)

The adsorptive capacity and kinetic data of three types of charcoal and three types of manganese dioxide for aqueous solutions of uric acid were studied. Two arrangements were used: the stirred-batch and the one using a column. The comparison for the x/m values between the two arrangements used, showed that the adsorptive capacity at the equilibrium concentration for the first arrangement is much lower than that of the second and the x/m values for the charcoals are 15 times lower than that of manganese dioxide.

Key words: uric acid, hemoperfusion, manganese dioxide, charcoal.

Introduction

With this report we would like to communicate experimental data on the adsorptive capacity of three different types of charcoal and three different types of manganese dioxide (MnO_2) for aqueous solutions of uric acid. Furthermore, we like to show the use of MnO_2 as an adsorbent of uric acid during hemoperfusion.

In recent years there have been several review articles[1] on the adsorption of uric acid from plasma solutions by δ-MnO_2. On the other hand, activated carbon has been used during hemoperfusion to adsorb uric acid and other substances while being in significant quantities in plasma in cases of chronic renal failure[2,3,4].

In our experiments, we study the ability of the carbons and the manganese dioxides to adsorb uric from aqueous solutions. In future work the conclusions will be compared with those of plasma solutions, to determine on the hemoperfusion conditions on one hand and the binding way of uric acid in plasma, on the other.

Materials and method

A. The uric acid solutions used, were prepared by diluting 1g of uric acid (Carlo Erba purity grade 99%) and 0.3g lithium hydroxide (LiOH) to 1000 ml with distilled water. Lithium hydroxide is used to dissolve uric acid in order to have it as anions. So the adsorbate is in the uric anion form. A quantity of 160 ml of the solution, having a concentration in uric acid 5.948×10^{-3} mol/1 was diluted to 1000 ml with distilled water. The concentration of the new solution has been estimated and found to be 0.8×10^{-3} mol/1 with a pH value 9.45. The concentration value was checked from time to time and it was quite constant.

The adsorbents used were:

1) Activated carbon (Merck N° 9624) particle size 0.5-0.75 mm.

2) Activated carbon (Norit N.V. Nederland and Grade Box 0.8 USP purity grade).

3) Activated carbon (BAC-MU Taiye kaken Co., Hykanin Che-Shinjuku-ku, Tokyo) particle size 0.8-1.2 mm.

4) β-MnO_2 prepared in our laboratory[5], particle size 0.05-0.1 mm.

5) γ-MnO_2 prepared electrolytically (TEKOSHA Co), particle size <0.0071mm.

6) δ-MnO_2 prepared in our laboratory[6], particle size <0.1 mm.

B. We followed two arrangements to study the adsorption: the stirred-batch and the one using the column.

For the stirred-batch arrangement we used 250 ml uric acid solution with a concentration of 0.8×10^{-3} mol/1 and 1g of charcoal or O.1g of MnO_2. The flasks were agitated at a temperature of 25°C with the help of a suitable arrangement. Samples of 0.5 ml from the supernatant were taken after 1, 2, 3, 15, 23 and 27 hours.

For the column arrangement we prepared a solution with the same concentration which we let to pass through the column. The column was placed vertically, being supplied from the lower end and the overflow was collected from the upper end. The uric acid solution was placed in a tank at a higher level (2 m) in order to have the necessary static pressure which overcomes the flow resistance of the column. The features of the columns for the different types of the adsorbents were:

Features of the columns	Carbons			MnO_2	
	Merck	Norit	BAC	γ	δ
1) Column diameter in cm	1.2	1.2	1.2	0.5	0.5
2) Column height in cm	4.1	3	3.9	0.4	0.1
3) Absorbent weight in g	1.85	1.95	2.66	0.155	0.058
4) Mean proportional velocity in ml/min.	1.85	1.74	2.35	0.24	0.87
5) Contact time of the adsorbate with the adsorbent in min.	1.64	1.28	1.28	0.25	0.07

where, mean proportional velocity (v_{MPV}) is the ratio between the Q_{total} in ml to the sum of partial times and Q_{total} is the sum of the products of the partial flow velocities X the corresponding times.

Contact time in min is the ratio between the free space which is left by the adsorbent in the column to the v_{MPV}.

The type β-MnO_2 as an adsorbent was not used in the column arrangement because we noticed from the experiments of the stirred-batch that it had a very low adsorptive capacity compared with the other types.

Analysis

The determination of uric acid to the solutions before, during and after the adsorption is made according to the Pileggi[7] method photometrically.

We estimate the adsorptive capacity of the different adsorbents from the results of the concentrations in samples in relation with the time; when x/m values

become independent with the time we say that the system has reached the equilibrium concentration.

In order to exclude the presence of Mn ions in plasma due to ion exchange, we determine Mn concentration in solutions before and after adsorption. The determinations are made after wet digestion of the samples and aspiration to an atomic absorption spectrometer, according to the Perkin-Elmer technical manual method for manganese.

Results and conclusions

A. At first we studied the stirred-batch arrangement. The solution being adsorsbed was: 250 ml uric acid solution made alkaline with lithium hydroxide. The concentration of the solution was 0.8 mm ol/1 with a pH value 9.45 at a temperature of 25° C.

The results are given in the following table I.

TABLE I. *Kinetic study of the adsorption on charcoals and MnO_2 of uric acid with the stirred-batch arrangement.*

Adsorbents		Uric acid sorbed per g of the adsorbent in mmol/g at times						Equilibrium concentration
Type	Quantities in g	$1^{st}h$	$2^{nd}h$	$3^{rd}h$	$15^{th}h$	$23^{d}h$	$27^{th}h$	of uric acid in mmol/1
1.C_{MERCK}	1	0.096	0.182	0.195	0.198	0.198	0.199	0.0060
2.C_{NORIT}	1	0.140	0.170	0.185	0.196	0.197	0.197	0.0100
3.C_{BAC}	1	0.083	0.127	0.144	0.186	0.191	0.195	0.0148
4. β-MnO_2	0.1	0.110	0.105	0.103	0.230	0.330	0.260	—
5. γ-MnO_2	0.1	1.450	1.670	1.750	1.960	1.890	1.990	0.0025
6. δ-MnO_2	0.1	1.212	1.700	1.790	1.860	1.870	1.870	0.0024

We observe in table I that x/m values at equilibrium concentration for all the types of the charcoal are the same, while the time they reach equilibrium concentration is shorter for the Merck charcoal, next for the Norit charcoal and last for the BAC one. This rate can be attributed to the differences of the particle size of the adsorbents. So we can say that the x/m values at the 27th hour are the values at the equilibrium concentration for all the adsorbents with the exception of β-MnO_2. As far as β-MnO_2 is concerned, its x/m value has not reached the equilibrium concentration under the conditions of this experiment, so it can not be compared to the other types of MnO_2. The comparison of x/m values between γ-and δ-MnO_2 at equilibrium concentration shows that the values are about the same.

Generally we can say from table I that x/m values for the diferent types of charcoal are about ten times lower than those for the different types of MnO_2.

In table II we observe that x/m values for the Merck's and Norit's charcoals are the same while for the charcoal of BAC is lower. These results on the adsorptive capacity must be correlated with the features of the columns. The higher adsorptive capacity for the Norit's charcoal against that of the BAC can be attributed to the fact that the v_{MPV} of the first (1.74 ml/min) is lower than that of the second (2.35 ml/min). The comparison between these two charcoals must be done with the same flow features.

TABLE II. *Kinetic study of the adsorption of uric acid on different types of charcoal and MnO_2 with the column arrangement.*

Adsorbents Type	Quantities in g.	Quantities of uric acid sorbed per g of the adsorbent x/m in mmol/g which correspond to the volume of the solution of uric acid that passed the column.					The sum of the partial x/m for the total volume that passed the column.
		0-100 ml	100-250 ml	250-500 ml	500-750 ml	750-1000 ml	
1.C$_{MERCK}$	1.854	0.039	0.053	0.076	0.066	0.059	0.292
2.C$_{NORIT}$	1.954	0.035	0.050	0.074	0.068	0.064	0.293
3.C$_{BAC}$	2.663	0.029	0.043	0.066	0.056	0.044	0.238
		0-25 ml	25-50 ml	50-75 ml	75-100 ml	100-125 ml	125-150 ml	
4. γ-MnO_2	0.155	0.129	0.129	0.127	0.127	0.127	0.128	0.767
		0-50 ml	50-100 ml	100-150 ml	150-200 ml			
5. δ-MnO_2	0.058	0.564	0.379	0.300	0.256			1.499

As far as the comparison between Merck's charcoal and that of Norit's is concerned, we observe that with about the same v_{MPV} and a longer contact time for Merck's charcoal against that of Norit's, we have the same x/m value.

As a conclusion we can say that Norit's charcoal has a higher adsorptive capacity than that of Merck's.

The comparison of x/m values between γ-MnO_2 and δ-MnO_2 is based upon flow data where the final conditions of the flow have not been achieved because of the column dimensions. The used dimensions were necessary because of the significant friction resistance of the adsorbents with respect to the specific arrangement used for the supply of the columns. With these experimental data we can say that δ-MnO_2 x/m value is higher than that of γ-MnO_2 x/m value when the same fluid quantities (150 ml) have passed.

The comparison for the x/m values between charcoal and MnO_2 shows that for the same fluid quantity that passed through the column the MnO_2 x/m values are 15 times higher than those of the charcoals.

The comparison for the x/m values between the stirred-batch arrangement and the one using the column, shows that the adsorptive capacity at the equilibrium concentration for the first arrangement is much lower than that of the second although equilibrium has not been achieved and of course the exhausting of the column. This is explained by the Freundlich equation.

Mn release

The release of Mn ions was checked in the adsorption systems with MnO_2 as an adsorbent; we did not find any Mn ions in all the samples tested.

Περίληψη

Συγκριτική μελέτη τῶν δεδομένων τῆς προσροφήσεως τοῦ Οὐρικοῦ ὀξέος πάνω σὲ διάφορους τύπους ἐνεργοῦ Ἄνθρακος καὶ Ὀξειδίων τοῦ Μαγγανίου

Στὴν ἐργασία αὐτὴ μελετᾶται ἡ προσρόφηση τοῦ οὐρικοῦ ὀξέος ἀπὸ

ὑδατικὰ διαλύματα ἐπάνω σὲ τρεῖς διαφόρου προελεύσεως προσροφητικοὺς ἄνθρακες (MERCK, NORIT, BAC) καὶ τρεῖς τύπους ὀξειδίων τοῦ μαγγανίου (β-MnO_2, γ-MnO_2, δ-MnO_2). Ὁ σκοπὸς τῆς μελέτης εἶναι νὰ προκύψουν δεδομένα ποὺ θὰ ἦταν χρήσιμα γιὰ τὴν ἀνάπτυξη τεχνικῆς γιὰ τὴν παραλαβὴ τοῦ οὐρικοῦ ὀξέος ἀπὸ βιολογικὰ ὑγρὰ δηλαδὴ μὲ αἱμοκάθαρση ἀπὸ προσροφητικὴ στήλη (HEMOPERFUSION).

Ἡ συγκέντρωση τῶν ἀλκαλοποιημένων μὲ LiOH ὑδατικῶν διαλυμάτων τοῦ οὐρικοῦ ὀξέος ἦταν 0.8×10^{-3} mol/1 καὶ τὸ pH:9.45

Ἀκολουθήσαμε δύο διατάξεις γιὰ τὴ μελέτη τῆς προσροφήσεως τὴν ἁπλὴ ἀνατάραξη καὶ τὴν προσροφητικὴ στήλη. Μὲ τὴ διάταξη τῆς ἁπλῆς ἀναταράξεως καὶ σὲ μελέτη κινητικῆς εὑρέθη ὅτι οἱ τρεῖς ἄνθρακες παρουσιάζουν τὴν αὐτὴ περίπου ἱκανότητα προσροφήσεως ἀνὰ γραμμάριο προσροφητικοῦ (πίνακας 1).

Γιὰ τὰ ὀξείδια τοῦ μαγγανίου στὸ ἀντίστοιχο μὲ τὸ προηγούμενο πείραμα εὑρέθη ὅτι τὸ β-MnO_2 προσροφᾶ πολὺ λιγώτερο ἀπὸ τὰ γ- καὶ δ- ὀξείδιά τους καὶ παρουσιάζουν ἱκανότητα προσροφήσεως κατὰ δέκα φορὲς μεγαλύτερη ἀπὸ αὐτὴ τῶν ἀνθράκων (πίνακας I).

Μὲ τὴ διάταξη προσροφήσεως σὲ στήλη καὶ μὲ προσροφητικὰ τοὺς ἄνθρακες οἱ τιμὲς τῆς ἱκανότητας προσροφήσεως ἦταν 0.292, 0.293 καὶ 0.238 mmol/g γιὰ τοὺς ἄνθρακες MERCK, NORIT καὶ BAC ἀντιστοίχως ὅταν ἀπὸ τὴ στήλη αὐτὴ ἔχει διέλθει 1 l διαλύματος οὐρικοῦ ὀξέος. Τὰ χαρακτηριστικὰ τῶν στηλῶν καὶ οἱ συνθῆκες ροῆς δίδονται σὲ πίνακα.

Στὶς στῆλες μὲ προσροφητικὰ τὸ γ- καὶ τὸ δ- ὀξείδια τοῦ μαγγανίου ἡ ἱκανότητα προσροφήσεως εἶναι 0,767 καὶ 1.243 mmol/g ἀντιστοίχως ὅταν ἔχει διέλθει ἀπὸ τὴ στήλη διάλυμα 150 ml οὐρικοῦ ὀξέος. Ἡ ἀπόλυτη σύγκριση τῶν τιμῶν x/m ἀπὸ τὴ διάταξη μὲ στήλη καὶ προσροφητικὰ τοὺς ἄνθρακες καὶ τὰ ὀξείδια τοῦ μαγγανίου δὲν εἶναι δυνατὴ ἐξ αἰτίας τῶν διαστάσεων καὶ τῶν συνθηκῶν ροῆς τῶν πειραμάτων. Πάντως μὲ τὰ δεδομένα αὐτὰ προκύπτει ὅτι ἡ ἱκανότητα προσροφήσεως εἶναι 15 φορὲς μεγαλύτερη ὅταν ὡς προσροφητικὸ χρησιμοποιεῖται τὸ ὀξείδιο τοῦ μαγγανίου.

Ἡ ἀναζήτηση ἐλευθερουμένων ἰόντων μαγγανίου στὸ διάλυμα ποὺ πέρασε τὴ στήλη ἦταν ἀρνητική.

Τὰ πειράματα αὐτὰ ἐνθαρύνουν τὴ μελέτη παρομοίων πειραμάτων γιὰ νὰ ἀναζητηθοῦν οἱ συνθῆκες ἐφαρμογῆς τῆς προσροφήσεως τοῦ οὐρικοῦ ὀξέος ἀπὸ αἷμα σὲ διατάξεις αἱμοκαθάρσεως.

References and Notes

1. Nathanael B.K., Tsoukali-Papadopoulou E. and Papadimitraki-Nathanael, A.: "The adsorptive capacity of δ-MnO_2 in the technic for the withdrawal of Pb from biological liquids", presented at the 3rd annual Greek Medical Meeting organized by Athens medical association, Athens, Hilton 5-7 of May 1977.
2. Denti, E., *et al* "Adsorbents in hemoperfusion", Kidney International vol. 7, p. S-401-S-405 (1975).
3. Yatzidis, H., Yulis G. and Digenis P., "Hemocarboperfusion-hemodialysis treatment in terminal renal failure", Kidney International, vol. 10, p.S-312-S-314 (1976).
4. Davis, Th., "Activated carbon fibers in hemoperfusion devices", Kidney International, vol. 7, p.S-406-S408 (1975).
5. Lux, H.: In Bauer's Handbook of preparative Inorganic Chmistry, vol. II, 2nd Ed. p. 1458, Academic Press, London (1965).
6. Buset, W., P. Graf. W., Fejtknect: *Helv. Chem. Acta*,**37**, 2322-28 (1954).
7. Pileggi, Vj., Di Giorgio J, Wybenga Dr: *Clin. Chem. Acta*., **37**: 141, (1972).

Chimika Chronika, New Series, 7, 221-227 (1978)

NUCLEAR QUADRUPOLE RESONANCE STUDY OF CRYSTALLINE HYDROGEN-BONDED COMPLEX BETWEEN 4-METHYLPYRIDINE AND DICHLOROACETIC ACID

E. HADJOUDIS, AND F. MILIA
Chemistry and Physics Departments
Nuclear Research Center "Demokritos", Athens, Greece.
(Received February 17, 1978)

Summary

The crystalline hydrogen-bonded complex between 4-methylpyridine and dichloroacetic acid was studied by the Nuclear Quadrupole Resonance (NQR) technique. The changes in NQR ^{35}Cl frequencies brought about by the complexation were investigated using conventional methods while for the weak ^{14}N frequencies the proton-nitrogen cross relaxation technique in the laboratory frame involving magnetic field cycling was used.

Key words: N.Q.R. Studies of Solids, Hydrogen bonding in Solids, Charge Transfer Complexes.

Introduction

The NQR method is very effective in studies on solid charge-transfer complexes since the transfer of an electron from a higher occupied molecular orbital of the donor to a lower vacant molecular orbital of the acceptor is accompanied by a change in electron distribution and a corresponding change in the electric field gradient at a particular atomic nucleus of the complex.

The hygrogen bond can be visualised also to be of the donor-acceptor type.[1] Among systems with hydrogen bonds, complexes of various chlorine-containing acids (CCl_3COOH, HCl), or other acceptors like chloranil with various donors have been examined by the NQR technique.[2,3]

The transmission of the effect of complex formation to the halogen atoms of the acceptors is achieved by an inductive mechanism and results to an increase of the ionic character of the C-Cl bond. For this reason the quadrupole spectra of the halogen containing acids should exhibit a low-frequency shift.

Although no other nucleus has as often been studied by NQR as ^{35}Cl, its role in NQR studies of hydrogen bonding is much smaller than ^{2}H, ^{17}O or ^{14}N. This is due to the smaller importance of the Cl-H---Y hydrogen bonds as compared to the OH---O or N--HO bonds. However, ^{35}Cl NQR has demonstrated its usefulness as a complementary tool in solving many special problems involving hydrogen bonding as in the case of chloral hydrate.[4]

In contrast to the case of ^{35}Cl NQR, the field of ^{14}N quadrupole resonance is relatively novel and its potential for the study of hydrogen bonding is just now being discovered. However, many N-H--0 and N-H--N resonances lie in the region between 800 KHz and 4.5 MHz which is hard to measure by classical NQR but double-resonance methods have opened this field for systematic investigations.

The present work deals with the hydrogen-bond strength and electronic distribution in a crystalline complex between dichloroacetic acid and 4-methylpyridine.[6] This complex contains both ^{35}Cl and ^{14}N nuclei and we used, in order to determine the NQR frequencies, convensional NQR methods for ^{35}Cl and the proton-nitrogen cross relaxation technique in the laboratory frame, involving magnetic field cycling[7] for the weak ^{14}N resonances of the complex.

Experimental

Compounds

The crystalline complex between dichloroacetic acid and 4-methylpyridine was prepared according to published procedures.[6] Recrystallisations, melting point (74° in agreement with literature[6]), and elemental analysis were used in order to verify the purity of the complex. The 4-picoline used was of 98% purity from Aldrich (Belgium).

Techniques

The ^{35}Cl quadrupole resonances were observed using the DECCA NQR spectrometer. Half to one gram samples were sealed in glass tubes of 1cm diameter and positioned in the spectrometer coil. The NQR spectra were obtained between 77 and 300 K.

Frequency measurements were accurate to ± 0.001 MHz and temperature measurements to ±1°C.

To determine the weak ^{14}N resonances in the complex, the proton-nitrogen cross relaxation technique in the laboratory frame, involving magnetic field cycling, was used.

I.v. absorption spectra were recorded on a 521 Perkin-Elmer spectrometer. The complex was examined in a KBr matrix.

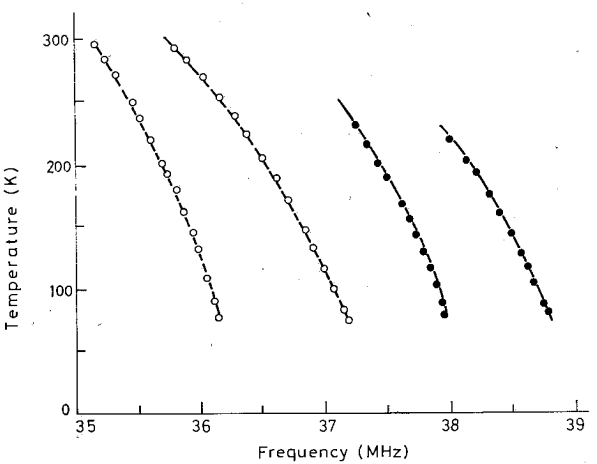

FIG. 1. *Frequency versus temperature curves of dichloroacetic acid and complex between dichloroacetic acid and 4-methylpyridine (-0-).*

Results

^{35}Cl frequencies

Fig. 1 shows the ^{35}Cl frequencies of the acceptor (dichloroacetic acid) and of the complex from room temperature down to liquid nitrogen temperature. It is seen that the chlorine frequencies in the complex are shifted to lower fields and the separation between the two chlorine atoms becomes greater. Table I summarizes the results for 77 and 196K.

Table I. *^{35}Cl resonance frequencies (in MHz)*

Compound	77K	Δν	196K	Δν
	37.979		37.475	
$CHCl_2$ COOH		0.828		0.721
	38.807		38.196	
	36.150		35.735	0.825
(C_6H_7N, $CHCl_2COOH$)		1.030		
	37.180		36.560	

Theoretical calculations

We decided to carry out some theoretical calculations in order to determine the electronic distribution in the complex with respect to dichloroacetic acid.

For nuclei with I = 3/2 the nuclear quadrupole resonance frequency is given by

$$\nu \pm \frac{1}{2} \rightarrow \pm \frac{3}{2} = \frac{e^2Qq}{2h}\left(1 + \frac{n^2}{3}\right)^{1/2} \qquad 1$$

and therefore e^2Qq and n cannot be obtained from pure quadrupole spectrum alone, since only one frequency is present.[8] Since n has not been determined by the Zeeman effect because of lack of sufficient large single crystals of chloroacetic acid, n is taken zero. However for halogen atoms $n<0.2$, and this gives rise to only slight changes in frequency.[9] The ν value of atomic chlorine is 54.873 MHz. The "p-electron defect" f is defined as

$$f = \frac{e^2Q_qMOL}{e^2Q_qAT} = \frac{\nu MOL}{\nu AT} \qquad 2$$

and therefore we can proceed to calculate the s hybridization in the C-Cl σ bond (s^2), the ionicity (I), and the functional double bond character (Π), using the frequency of dichloroacetic acid at 77° K from equation 3.

$$e^2Qq_{MOL} = -(1 - s^2 - I - \Pi)\, e^2Qq_{AT} \qquad 3$$

For the C-Cl bond, Das and Hahn[8] give $s^2 = 0.15$ and I = 0.190. To calculate Π we use the semiempirical rule proposed by Pauling.[10] According to this rule

$$\Pi = (R_1 - R_0)/(R_1 + 2R_0 - 3R_2) \qquad 4$$

where R_1 and R_2 represent the bond distances for single and double bonds between the two atoms, and R_0 is the observed distance. The distance R_1 and R_2 may be obtained from the singly and doubly bonded covalent radii of atoms that have been tabulated by Pauling.[10] Using R_1 = 1.76 A, R_2 = 1.56 A and R_2 = 1.75 A

(estimated) we get $\Pi = 0.017$. Substitution of these calculated values in eqs. 3 and 2 gives a theoretical f - 0.643 compared with the observed values for the two chlorine atoms (called Cl(1) and Cl(2), $f_{Cl(1)} = - 0.692$ (37.979 MHz/54.873 MHz) and $f_{Cl(2)} = - 0.707$ (38.807 MHz/54.873 MHz). If we assume $\Delta s^2 = 0$ and $\Delta\Pi = 0$ (that is, the s and Π character remain the same), we find that $I_{Cl(1)} = 0.174$ and $I_{Cl(2)} = 0.155$. This indicates that the degree of charge transfer is approximately 9.0% as experienced by the Cl(1) atom and 22.5% as experienced by Cl(2) atom in dichloroacetic acid.

^{14}N frequencies

In 4-methyl-pyridine the ^{14}N NQR frequencies were measured at 77 and 190 K using convensional NQR spectroscopy and were found to be

at 77K
$$\nu_{+} = \frac{3}{4h} e^2qQ \left(1 + \frac{1}{3} n\right) = 3.6884 \text{ MHz}$$
$$\nu_{-} = \frac{3}{4h} e^2qQ \left(1 - \frac{1}{3} n\right) = 2.9327 \text{ MHz}$$

at 190 K
$$\nu_{+} = 3.6484 \text{ MHz}$$
$$2.9121 \text{ MHz}$$

in agreement with previous measurements.[11] From the above values the ^{14}N quadrupole coupling constant and the asymmetry parameter were evaluated as

$$e^2qQ/h = \frac{2}{3} (\nu_{+} + \nu_{-}) = 4414 \text{ KHz}, \; n = 0.34 \; (77K)$$

and
$$e^2qQ/h = \frac{2}{3} (\nu_{+} + \nu_{-}) = 4373 \text{ KHz}, \; n = 0.33 \; (190K).$$

In the complex between dichloroacetic acid and 4-methylpyridine, the pure ^{14}N NQR transitions was not possible to be detected with convensional NQR spectroscopy and they were determined, using the proton-nitrogen cross relaxation technique in the laboratory frame, from the observed spectrum (at 190 K) shown in Fig. 2 as

$$\nu_{+} = \frac{3}{4h} e^2qQ \left(1 + \frac{1}{3} n\right) = 1190 \text{ KHz}$$

$$\nu_{-} = \frac{3}{4h} e^2qQ \left(1 - \frac{1}{3} n\right) = 935 \text{ KHz}$$

$$\nu_{0} = \frac{1}{2h} e^2qQn = 255 \text{ KHz}$$

so that the ^{14}N quadrupole coupling constant e^2qQ/h and the asymmetry parameter

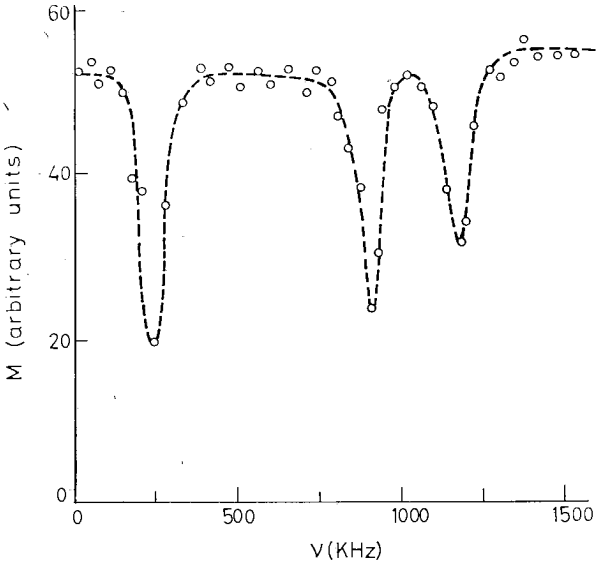

FIG. 2. *Proton-nitrogen cross-over relaxation spectrum of complex between dichloroacetic acid and 4-methylpyridine at T = 190K.*

n could be determined as

$$e^2qQ/h = \frac{2}{3}(\nu_+ + \nu_-) = 1420 \text{ KHz}$$

$$n = 0.36$$

I.r. spectrum

The solid state spectrum of the 4-methylpyridinedichloroacetic acid complex shows the $V_{CO_2^-}$ band at 1640 cm^{-1} and two V_{N^+H} bands at 2460 and 2110 cm^{-1}.

Discussion

In pure dichloroacetic acid two frequency lines are observed in agreement with previous observations.[12] The temperature dependence of the frequencies (Fig. 1) in qualitative agreement with the theory of Bayer.[13] The lines present no discontinuities from room temperature down to liquid nitrogen temperature showing that no phase transformations occur. The two frequencies are separated by about 0.8 MHz in the pure compound and by about 1 MHz in the complexed. These values are too large to be caused by crystallographic differences only but in this case the decision as to the cause must await a crystal structure determination of the dichloroacetic acid. However, the observed shift of ^{35}Cl frequencies to lower fields and the theoretical calculations indicate charge transfer to the acceptor ($CHCl_2COOH$) that is oxygen and chlorine gain charge density. The values estimated for the transfer (9.5% and 21.7% as experienced by the two chlorine

atoms) may be small but it should be remembered that in this complex (I) the chlorine atoms in dichloroacetic acid are secondarily affected by the charge transfer.

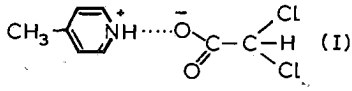
(I)

However, the picture is completed if we examine the results with ^{14}N frequencies. First we notice that only one chemically non-equivalent ^{14}N site per unit cell could be detected in both cases (pure 4-methylpyridine and complexed) and second the magnitude of the ^{14}N quadrupole coupling constant in the complex is dramatically lower than in the pure 4-methylpyridine (1420 KHz against 4373 KHz), thus demonstrating not only a very strong hydrogen bond but that a proton transfer has occured and (I) is actually a crystalline ion pair species. These results are in agreement with the order of magnitude found for the coupling constants for the N and N-H groups in solid imidazoles and related compounds by Edmonds and his co-workers.[14]

The i.v. results are also in favor of the ion pair species showing the N^+H band in agreement e.g. with salts of pyridine indolene and Schiff's bases in which the group C=N+H- absorbs in the same region.[15]

Acknowledgements

We would like to thank Prof. R. Blinc for inviting one of us (F.M.) in the University of Ljubljana "J. Stefan" Institute for measurements with the proton-nitrogen cross relaxation technique.

We would like to thank also Mr. M. Voudouris for his skilful assistance throughout the work.

Περίληψη

Μελέτη τοῦ κρυσταλλικοῦ συμπλόκου μεταξὺ 4-μεθυλοπυριδίνης καὶ διχλωροοξεικοῦ ὀξέως μὲ τὴν μέθοδο τοῦ πυρηνικοῦ τετραπολικοῦ συντονισμοῦ.

Μελετήθηκε μὲ τὴν τεχνικὴ τοῦ πυρηνικοῦ τετραπολικοῦ συντονισμοῦ (NQR) τὸ κρυσταλλικὸ σύμπλοκο ποὺ σχηματίζεται μεταξὺ 4-μεθυλοπυριδίνης καὶ διχλωροοξεικοῦ ὀξέος. Οἱ μεταβολὲς στὶς συχνότητες NQR τοῦ ^{35}Cl τοῦ διχλωροοξεικοῦ ὀξέος, μετὰ τὴν συμπλοκοποίηση, μελετήθηκαν μὲ τὴν συμβατικὴ τεχνικὴ τοῦ NQR ἐνῶ γιὰ τὶς ἀδύνατες συχνότητες τοῦ ^{14}N τῆς 4-μεθυλοπυριδίνης χρησιμοποιήθηκε ἡ τεχνικὴ τῆς διασταυρουμένης ἐφησυχάσεως πρωτονίου-ἀζώτου.

Βρέθηκε ὅτι τὸ κρυσταλλικὸ σύμπλοκο σχηματίζει ἀρκετὰ ἰσχυρὸ δεσμὸ ὑδρογόνου ὥστε νὰ θεωρεῖται ὅτι βρίσκεται σὲ ἰοντικὴ κατάσταση.

References and Notes

1 Mulliken, R.S., *J. Chim. Phys.,* **61**, 20 (1964).
2 Bennet, R.A., and Hooper, H.O., *J. Chem. Phys.,* **47**, 4855 (1967).
3 Hadjoudis, E., Ward, T.A., and Milia, F., "Proceedings of the Second International Symposium on NQR Spectroscopy", Ed. A. Colligiani, A. Vallerini Publisher, Pisa, Italy, 1975.
4 Milia, F., and Hadjoudis, E., *J. Phys. Chem.,* **74**, 1642 (1970).
5 Blinc, R., *Magnetic Resonance Studies of Hydrogen Bounding in Solids* in "The hydrogen bond-recent developments in theory and experiments" p. 857 Eds. Schuster, P., et al. North-Holland Publ. Co., Amsterdam, 1976.
6 Dega, - Szafram, Z., Grech, E., Naskret-Barciszowska, M.Z., and Zafram, M., *J. Chem. Soc.,* (Perkin II), 250 (1975).
7 Seliger, J., Osredkar, N., Mali, M., and Blinc, R., *J. Chem. Phys.,* **65** 2887 (1976).
8 Das, T.P., and Hahn, E.L., "Nuclear Quadrupole Resonance Spectroscopy", Academic Press Inc. Publishers, New York, London, 1958.
9 Maksyutin, Yu. K., Guryanova, E.N., and Semin, G.K., *Russ. Chem. Rev.,* **39**, (4) 334 (1970).
10 Pauling, L., "Nature of Chemical Bond", p. 164 Cornell University Press, Ithaca, N.Y., 1948.
11 Birynkov, I.P., Voronkov, M.G., and Satin, I.A., "Tables of NQR Frequencies" p. 113, Israel Program for Scientific Translations, Jerusalem 1969. Guibe, L., *Ann. Phys.,* **7**, 177 (1962).
12 Allen, H.C., Jr., *J. Am. Chem. Soc.,* **74**, 6074 (1952).
13 Bayer, H., *Z. Physik,* **130**, 227 (1951).
14 Hunt, M.J., Mackay, A.L. and Edmonds, O.T., *Chem. Phys. Letters,* **34**, 473, (1975).
15 Bellamy, L.J., "The Infra-red Spectra of Complex Molecules", p.260, Methuen; Co Ltd, London, 1960.